Microfluidic Lab-on-a-Chip

Final Design Report

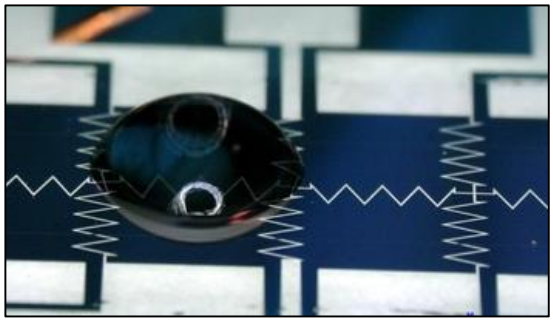
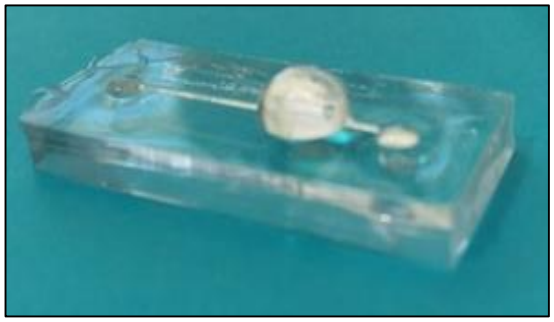
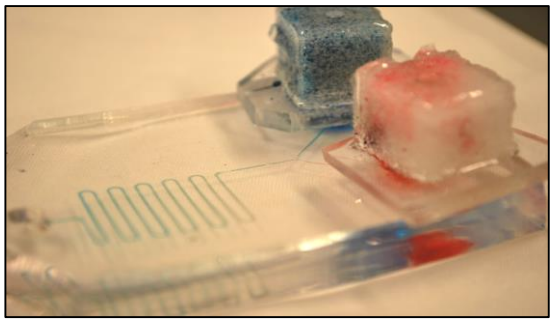
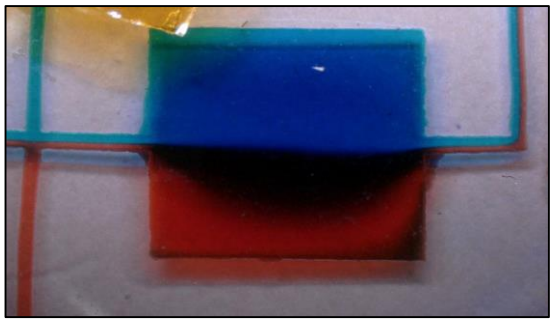

Project Team:
Samuel Feinman
Erika Hancock
Christopher Stolinski
Bryan Tran

Project Advisor:
Brian Baker

Project Sponsors:
W.M. Keck Foundation

Approval:

_____ Date: _____
Brian Baker

Table of Contents

1. Executive Summary

1.1 Introduction

The world of microscale engineering is growing in many fields, including medical, semiconductor, military, security, and energy industries. It is estimated by the National Nanotechnology Infrastructure Network that by the year 2020 the United States market value of products using micro/nanoscale technology will be 5% of the GDP - about one trillion dollars ("Nanotechnology Careers" n.d). As the demand for engineers in microscale engineering increases, the importance of introducing young students to microscale phenomenon becomes paramount. In order to make an indelible impact on students, concepts of physical phenomena on the microscale should be introduced in an interactive and demonstrative manner, as opposed to a traditional lecture format. A study conducted by the Department of Physics at Indiana University (Hake 1998) showed that students who were taught basic physics concepts in an interactive, hands-on manner had a better understanding of the material and performed better on exams. Interactive devices and teaching modules were created to explain scaling laws and practical applications in microfluidic systems.

1.2 Target Market

The target market for these teaching modules include high school and college level physics, engineering, and technology instructors and, ultimately, their students. Many of these instructors may not have a fundamental understanding of microscale engineering, but the teaching modules will include reference material so that they feel comfortable teaching students the concepts. The students will then be able to interact with the lab-on-a-chip (LOC) devices and experience the physical phenomenon that are prominent at a small scale. The modules will also include presentation slides for the instructors and students to view, elucidating on each device.

1.3 Key Project Focus Areas

The focus of this project is to create eight LOC devices that demonstrate myriad scaling effects in microfluidics, along with real-world applications. These scaling effects and applications include, but are not limited to, micro-droplet formation, polydimethylsiloxane (PDMS) pumps, gradient mixers, PDMS lens, hydrophobic PDMS cubes, micro pin valves, capillary action, and electrowetting. Each LOC will be interactive and affordable to fabricate, and will be accompanied by background information describing each chip and a set of presentation slides to be displayed alongside the devices.

1.4 Conclusion

Considering all of the needs of the customers - teachers and students - an assortment of eight LOC devices will be designed, fabricated, and packaged to send to high school and college laboratory classes. The LOCs will introduce students to the effects of scaling laws on physical phenomena in microfluidic devices, as well as real-world applications of the phenomena the devices exhibit. In order to accomplish the teaching aspect of the devices, each LOC device will be accompanied by background material and presentation slides.

2. Context

2.1 Needs

Engineering applications are continuously getting smaller, and in the field of micro-engineering, specifically microfluidics, scaling-down technologies affect physical and fluidic properties that do not conform to the observable, macro-world. Many micro and nano engineering classes are taught solely with projector-based lectures with little to no real-world demonstrations and interactions. This is akin to taking a freshman physics course without in-class demonstrations, which not only help prove, but also solidify complex ideas. This greatly affects the learning-retention of the students. In order to bring micro-observable phenomena to a viewable format, students and educators need access to low-cost, easy-to-use devices that demonstrate microfluidic phenomena in an educational and impressionable way. Academic institutions need LOC devices to instruct microfluidic phenomena properly.

2.2 Problem Statement

While many universities have the resources to teach fabrication processes and techniques, many are not geared for physical demonstrations of scaling laws on the micro-scale. This is due to the challenge of fabricating and designing simple, yet demonstrable, devices capable of showcasing microfluidic scaling laws. These scaling effects must be understood in order to design micro-fluidic devices. The scaling and real-world devices that will be fabricated are: micro-droplet formation, PDMS pumps, gradient mixing, PDMS lens, hydrophobic PDMS cubes, micro pin valves, capillary action, and electrowetting. Many challenges present themselves when working on the fabrication of micro-devices: design, manufacturability, fabricating working fluid channels, and bonding channels to a particular substrate. To overcome these challenges, numerous iterations of prototypes will be produced and tested to ensure proper channel function. Testing and research will be conducted to determine the optimal way to bond the channels - either glass or PDMS substrates. Overcoming these challenges is necessary to develop demonstrable and educational microfluidic LOC devices.

2.3 Design Team

The Microfluidic LOC Device team comprises four mechanical engineering undergraduate students. Each student has experience in cleanroom fabrication and has completed advanced coursework in micro-engineering. Each team member is responsible for designing and fabricating two devices, with the team ultimately producing eight chips that demonstrate various micro-scaling phenomena and real-world applications.

2.3.1 Student Design Team Members

Bryan Tran (Team Leader) – bryan.tran0912@gmail.com

Bryan has over two years of cleanroom experience through his work at the Utah Nanofab. Originally hired as a lab technician who assisted in maintaining the clean room and equipment, he moved into a position on a project to research and develop a simple in-house MEMS fabrication process. With the guidance of University of Utah faculty advisor, Brian Baker, Bryan and a team member designed a MEMS device that won a Sandia University Alliance design competition. Along with several relevant courses, such as micromachining, microsystems design and characterization, and solid-state physics of micro sensors, he has also acquired a degree emphasis in micro/nanoscale engineering.

Sam Feinman – samfeinman93@gmail.com
Sam has experience with micro fabrication techniques and technologies and has clean room experience, including the fabrication of a micro-heater. He has industry experience in facets of micro-engineering involving super-resolution, single-molecule localization microscopy at Bruker Nano Surfaces Inc. He has also taken advanced coursework in micromachining and fundamentals of micro/nanoscale engineering.

Erika Hancock – erihancock@gmail.com
Erika has cleanroom experience through her summer internship with IM Flash Technologies as well as her work as an equipment engineer at IM Flash since January. She has completed and advanced micro-engineering courses, including microfluidics, micromachining and fundamentals of microscale engineering. Erika has previous experience designing, fabricating, and testing microfluidic devices.

Christopher Stolinski – chris.stolinski@gmail.com
Christopher participated in a micro-engineering class that is focusing on scaling laws and fabrication. He is experienced in AutoCAD, used for the design of the microfluidic devices. Christopher has some experience in the clean room, but is excited to continue to learn as he works on this project.

2.3.2 Team Advisor
Brian Baker – bbaker@eng.utah.edu
Brian Baker received the B.S. degree in electrical and computer engineering from Brigham Young University in 1994 and an M.S. degree in electrical engineering from the University of Utah in 2000. He has seven years of industry experience as a MEMS process engineer. He has been a research associate during the past twelve years working in the Utah Nanofab in the College of Engineering at the University of Utah. He assists researchers and companies in the design and fabrication of various micro and nano devices. He has taught college courses on microfabrication, nanotechnology, and MEMS design. As a co-instructor of a micro-systems design class, he guided a team of students in designing a MEMS chip that won the Sandia University Alliance educational design competition. His research interests include microsensors, microactuators, microfluidics, NEMS and MOEMS. He is currently pursuing a PhD at the University of Utah. His research is in neural interfaces and is funded by a co-PI on a Keck grant to create educational microchips and materials that teach and demonstrate scaling engineering principles.

2.3.3 Corporate Liaisons and Sponsors
In early 2013, the Utah Nanofab received a generous grant from the W.M. Keck Foundation to research and develop engineering education material to teach the effects that scaling has on physical phenomena to college and high school students nationwide. Originally accomplished through the use of MEMS, the Nanofab has now shifted the residual funds from the grant to create material in microfluidics for a similar purpose.

3. Design Requirements

3.1 Design Overview

The LOC devices have two distinct customers: students and educators. The purpose of these LOCs are to be educational, demonstrable, and interactive, which requires numerous design elements to tailor both customers' needs. It is in the interest of the students for the design to be memorable and hands-on, to cement the phenomena they learn from the chip and to have them engaged in the lesson. For the educators, it is paramount that the LOCs are easy to setup and demonstrate, while also having proper learning material to teach microfluidic concepts. In order to determine the customer needs, a survey was generated for high school students to gauge their interest and knowledge of micro-engineering and preferred learning styles i.e. lectures, PowerPoints, and interactive demos. To gauge the needs of the educators, there was a question-and-answer session with the project advisor, Brian Baker, to determine specific needs of accompanying educational material. The end goal is to fabricate eight LOC devices that are designed to be unique, hands-on, and educational, while simultaneously being interchangeable, easy-to-use, easy-to-teach, and obtainable for any academic institution or educator.

3.1.1 Students

The students, who are high school and college-aged, will be using LOCs as interactive demonstrations. The LOCs will aid in securing a better understanding of microfluidic scaling concepts and phenomenon. This interaction will help solidify the learned scaling laws, as opposed to a projector-only presentation. Students will be more enticed to learn about microfluidics through hands-on experiences, which are currently unavailable on the mainstream market.

3.1.2 Educators

The LOCs will be an easy way for any science educator to approach the field of micro-engineering, regardless of their engineering background knowledge. The presentations that come with each chip will be informative and easy to both understand and teach. Educators will want this product due to its simplicity and educational value, along with being interactive, low-cost, and easily transportable.

Table 3.1. Primary and secondary needs to customers.

Primary Need	Secondary Need
Clearly demonstrate microfluidic scaling phenomena	Provide background information about engineering and fluid flow
	Accompanied by teaching material in non-technical language
	Use colored fluids to better show phenomena
	Design unique geometries to better engage the students
Interactive	All students can easily setup and/or exchange LOCs
	Students can adjust LOCs to see how changing parameters affects the device
Inexpensive	Easy to replace/manufacture devices
Properly packaged for distribution	Durable
Safe	No toxic fluids will be used
	Protected sharp corners or edges on LOCs

Table 3.2. Ranking of customer need.

#	Customer Need	Importance (1-5)
1	Clearly demonstrate microfluidic scaling phenomenon	5
2	Students can adjust LOCs to see how changing parameters affects the device	5
3	Easy setup for lab demonstration	5
4	Accompanied by teaching material written in non-technical language	5
5	Provide basic background information about engineering and fluid flow	4
6	Design unique geometries to better engage the students	4
7	Use colored fluids to better show phenomena	4
8	Easy to replace/manufacture devices	4
9	Durable	3
10	No toxic fluids will be used	3
11	Protected sharp corners or edges on LOCs	2

3.2 Demonstrate microfluidic scaling phenomenon

Most people have a fundamental understanding of how fluids behave on the macroscopic scale since interactions with these systems occur daily; however, when scaling-down fluidic systems, physics behaves in unexpected ways. The purpose of these LOC devices is to visually demonstrate non-intuitive microfluidic phenomena.

3.2.1 Provide basic background information and teaching material

Many students have not been exposed to the world of microfluidics, let alone engineering; therefore, background information will be presented to the students before they can interact with the LOCs. This background information will be broad, focusing on general properties of fluid flow and typical problems or jobs that an engineer would work on. This material will be written in non-technical language. The teaching material accompanying each chip will delve deeper into the scaling effects and specific physical properties relevant to the LOC. Equations and tables used during the design of each chip will be presented.

3.2.2 Use of colored fluids

The use of fluids such as water dyed with food colorings will aid in visualizing the phenomena on each LOC. Since the substrates, PDMS and glass, used to create the devices are clear, utilizing colorful fluids in the channels will maximize the viewing experience of the user.

3.2.3 Design of unique geometries

In order to engage students, unique geometries are incorporated into each LOC. Such features include intricate serpentine channels, viewing windows, or channels arranged to form a picture. When students see unexpected or fun geometries, a lasting impression of the presentation will be made, and the technical information will be better remembered.

3.3 Interactive

The point of the LOCs is that students can interact with a device and learn from it in an engaging manner. The interactive aspect of the device will increase the learning-retention rate by the students, which provides a higher chance of students remembering what they learned, as opposed to a teacher giving a PowerPoint lecture.

3.3.1 Easy setup and exchange

There will be eight LOC devices, and in order to minimize time spent exchanging devices and setting them up, or breaking a device due to challenging setup procedures, each device will be designed such that exchanging one chip for another will be seamless and clean. This will be done largely through the design of inlets and outlets on the chips.

3.3.2 Adjustable

In order for students to interact and change the fluid settings on the LOCs, minimal and ordered universal connections will be made to adjust fluid flow without spillage or causing damage to the devices.

3.4 Inexpensive

Micro-engineering technology is expensive, which is a primary reason that institutions do not offer interactive devices to teach students, especially in high school settings. Devices would most likely cost more than what a school would have in the budget for this type of lab. In order to accommodate any school's budget, the LOCs must be designed and fabricated in an inexpensive manner that is both high quality and can be easily manufactured.

3.4.1 Easy to replace/manufacture devices

In case a device breaks and needs to be replaced, it needs to be inexpensive to manufacture so the LOC can be replaced quickly and cheaply.

3.5 Properly packaged for distribution

The chips will be sent out to numerous schools and universities, and packaging is important to ensure that all LOCs can survive any shipping method or travel. It is also important that the devices be packaged in such a way that all devices are free of dirt and other impurities during travel or in classroom demonstration settings.

3.5.1 Durable

The LOCs must be able to withstand multiple tests, demonstrations, and travel, all of which effect of the chips will be designed and packaged. Durability during shipping is paramount when considering packaging design to keep the need of replacing an LOC low.

3.6 Safe

Safety is always a concern in engineering design, since it is never the intention of the designers to cause any harm to the end user. While the users, typically aged 15-25 years old, of the LOC devices are mature enough to avoid most sources of harm, extra care will be taken on the design end to prevent cuts, shocks, and unwanted exposure to liquids.

3.6.1 No toxic fluids used

While it is not expected that an end user would directly and purposefully ingest any of the fluids used in the LOC devices, there is the potential for fluids to contaminate the user's hands through the installation and removal of the tubing system, leaks, etc. Therefore, only non-hazardous fluids, like water, oils, and food coloring, will be used on the LOC devices. The capillary action device is the exception and is described more in section 4.9.3.

3.6.2 No sharp corners or edges

Some of the final LOC devices may be bonded to glass slides, which presents the possibility of cutting oneself on the edge of the slide. In order to prevent unwanted injury, care will be taken to cover these sharp edges and to warn users of the possibility of harm before they use the devices.

4. Design Specifications

4.1 Overview of Design Specifications

With eight different LOC devices, there are myriad design specifications, including overall specifications applying to each LOC as well as device-specific ones. In order to meet all of our customer's needs, marginal and ideal metrics have been assigned to an array of specifications that are related to a particular customer's needs. Table 4.1 shows the metrics, along with all of the LOC's corresponding needs, Tables 4.2 – 4.9 show specifications to individual devices, and sections 4.2 – 4.10 contain descriptions of the specifications. The metrics are organized starting with metrics that apply to all LOCs, and then the metrics for each device. The table is organized based on importance of the specification.

Table 4.1. Specifications for all LOC devices.

Metric	Customer Need	Specification	Units	Marginal	Ideal
1	7, 11	Non-hazardous fluids and materials	Rating #	NFPA Rating 0 - 3	0
2	3	Inlet port size	mm	2.0 – 3.0	3.0
3	3	Number of outlet ports	Integer	1	1
4	1, 2, 6	Interactive	Binary	-	-
5	3	Time for lab setup	min	20 ± 10	<15
6	1, 4, 5	Teaching material written in non-technical language for educators	1-10 Scale (survey)	7 – 10	>7
7	1, 6, 7	Unique and interesting designs for showing phenomenon	Binary	-	-
8	10	Low cost	$	30 – 50	30
9	8	Scalable fabrication	days	3 – 5	3
10	9	Able to withstand handling by students and educators	Binary	-	-
11	9, 10, 12	Packaging for ease of shipping	Binary	-	-

Table 4.2. Micro droplet formation.

Metric	Customer Need	Specification	Units	Marginal	Ideal
1	1, 2	Flow rate of fluid one	µL/h	440 ± 10	440
2	1, 2	Flow rate of fluid two	µL/h	440 ± 100	440
3	1	Viewing window dimensions	µm	>50x50	1000x700
4	1, 3	Number of inlet ports	Integer	>2	3

Table 4.3. PDMS pumps.

Metric	Customer Need	Specification	Units	Marginal	Ideal
1	9	Durable	Binary	-	-

Table 4.4. Gradient mixer.

Metric	Customer Need	Specification	Units	Marginal	Ideal
1	1, 3	Number of inlet ports	Integer	>1	2
2	1	Flow rate of mixing fluids	µL/min	50 ± 10	50
3[1]	1, 3	Effective mixing at center channel	%	80 – 100	100

[1] In reality, this metric will be visually measured, and is therefore somewhat subjective. Some quantification can come from the RGB value analysis to determine uniformity of color at the channel outlet.

Table 4.5. PDMS Lens.

Metric	Customer Need	Specification	Units	Marginal	Ideal
1	1, 3	Number of inlet ports	Integer	>1	2
2	1, 2, 10	Membrane thickness	µm	>100	100 – 200
3	1, 2	Radius of lens	cm	0.25 – 1	0.34
4	1, 2	Optical zoom	X	>10	>30

Table 4.6. Hydrophobic PDMS Cubes.

Metric	Customer Need	Specification	Units	Marginal	Ideal
1	1, 2	Surface roughness	-	-	-

Table 4.7. Micro Pin Valves.

Metric	Customer Need	Specification	Units	Marginal	Ideal
1	1, 2	Number of inlet ports	Integer	>1	3
2	1, 2	Number of pin valves	Integer	>4	12
3	1, 2, 6	Number of channels per inlet	Integer	>2	4
4[2]	1, 2	Channel width	µm	200 – 1000	200 – 1000
5	1, 2	Block or allow fluid flow	Binary	-	-

[2] This device will have a range of channel widths in order to maximize user interaction and demonstration potential, so there is no singular ideal width.

Table 4.8. Capillary action.

Metric	Customer Need	Specification	Units	Marginal	Ideal
1	1, 2	Number of inlet ports	Integer	>1	5
2	1, 2	Channel width	µm	50 – 300	100
3	10	Fluid type	-	-	-

Table 4.9. Electrowetting.

Metric	Customer Need	Specification	Units	Marginal	Ideal
1	10	Fluid type	-	-	-
2	6	Electrode size (area)	mm^2	2 – 5	3
3	1, 2	Activation voltage	V	80 – 120	110
4	1, 2	Droplet size	µL	2 – 5	2
5	8, 9	Durable	Binary	-	-

4.2 LOC Device Specifications

4.2.1 Use non-hazardous fluids and materials

It is imperative that each device is safe to handle in case of device leakage due to inlet or outlet ports breaking. Since the devices will be exchanged multiple times and fluid will be running through the devices constantly, it is necessary to make sure the fluid is safe in the following respective hazards: health, flammability, reactivity, and specific (acids, corrosive, oxidizer). The National Fire Protection Association (NFPA) created a quantitative scale (0 to 4, 0 being completely safe) that describes a material's hazard levels. Water, food coloring, and oils (olive, hexadecane) are used in the most of the LOCs, which rank 0 in health, flammability, and reactivity, meaning it is completely safe if liquid comes in contact with the user. The capillary action device is the only exception and, due to the nature of the device, must use isopropyl alcohol as a fluid which has a health rating of 1 and a flammability rating of 3, meaning it can cause minor skin irritation and is flammable under ambient conditions. Isopropyl alcohol, more commonly known as rubbing alcohol, is already included in nearly all first aid kits as a standard antiseptic. Thus, this fluid is safe to handle under normal conditions with the proper precautions: used with gloves and kept away from an ignition source.

4.2.2 Inlet port size

The devices will be interchangeable, and to make the process of switching out one LOC for another easy and clean for an instructor or student, each device will have the same inlet port size. Based on the diameter of the tubes used for the delivery of fluid to the device, a standard biopsy punch of 3 mm was selected.

4.2.3 Number of outlet ports

Since most of the devices involve continuously flowing fluid, the fluids need to be able to leave the chip cleanly. To simplify the process, each chip will have the same outlet setup: one outlet at the end of the chip. The same biopsy punch for the inlet ports will be used for these ports.

4.2.4 Interactive

The objective of these chips is to demonstrate microfluidic phenomenon in an engaging way. Each chip will be capable of being manipulated by the user, whether it is by changing fluid flow or activating a device.

4.2.5 Time for lab setup

The devices are meant to be simple demonstrations, which should be synonymous with a quick and simple setup procedure. For a first time user, it should take no longer than twenty minutes to get the first device up and running from start to finish. After the initial setup, it should only take minutes to switch out different devices. This is based on the amount of time it took each team member to setup each device from start to finish, including exchanging the devices. A few extra minutes were included to account for first time users.

4.2.6 Teaching material written in non-technical language for educators

Each respective LOC will come with easy-to-present and easy-to-digest presentations for the educators to give to the students. The presentation goes into the math, physics, and design of the LOCs and is easy enough to understand for a wide-range of students - freshmen in high school to seniors in college - to comprehend, yet informational enough to have a better understanding of microfluidic scaling laws. Measuring the understanding of the presentations will come from a short quiz given out at a trial run of the presentation to high school students, and, while every student should be able to score a 10/10, ideally the lessons can be considered learned if someone scores above a 7.

4.2.7 Unique and interesting designs for showing phenomenon

In order to make the LOCs memorable, each device will have a unique design without compromising its intended actions. This will help better teach the scaling laws by making the students remember the devices because of their distinguishing designs i.e. incorporating a "U" in the design and intricate channels.

4.2.8 Low cost

These devices will potentially be used in high school labs. Many schools have small budgets for labs, so inexpensive development is important, as per our tight-budgeted consumers. As of now, there is not a quantifiable number for cost, but as fabrication continues, it will be monitored to find areas to maximize efficiency and keep costs as low as possible.

4.2.9 Scalable fabrication

The LOCs should be able to be manufactured in no more than one workweek. This falls under the concern of being able to easily replace a damaged chip. The process for manufacturing a new device is fast, and should a customer request a specific chip, they should expect to get a new chip in a matter of days.

4.2.10 Able to withstand handling by students and educators

Since LOCs will be switched out and demonstrated multiple times, it is necessary to make each LOC durable and able to withstand many tests. All of the devices are interactive, thus making it paramount to have sturdy, reliable chips.

4.2.11 Packaging for ease of shipping

Each chip will be individually packaged in such a way that it will be clear of any contaminants during shipment and travel, sturdy to withstand said travel, and to properly store and organize the collection of LOCs.

4.3 Micro droplet Formation

The micro droplet device shows how flow rates can be modified to change droplet volume, and how micro droplets are used in real-world applications.

4.3.1 Flow rate of continuous fluid

The metric was determined based on research by Zhang and Wang (Zhang, Wang, 2011). The geometry of this device is different from the article so this metric will serve as a starting point. After further testing, the continuous flow fluid worked well at 440 μL/hr and will not need adjustment.

4.3.2 Flow rate of dispersed fluid

This flow rate was also based on research by Zhang and Wang (Zhang, Wang, 2011). The geometry of the device is different from in the article so this metric will serve as a starting point. After further testing it was determined that the flow rates of this fluid should be between 240 and 640 μL/hr. At this range of flow rates, it is possible to show how the rate of droplet formation can be changed and at the same time continuously form droplets.

4.3.3 Viewing window dimensions

The original dimensions used for the viewing window were determined from the same research noted above in specifications 4.3.1 and 4.3.2 (Zhang, Wang, 2011). However, the final device does not have a viewing window due to the last minute iterations made with the new geometry. Concern was focused on getting the device to form droplets, and there was not enough time for further iterations.

4.3.4 Number of inlet ports

There are three inlet ports and one outlet port in the micro droplet device. Two of the inlet ports are for the continuous flow fluid, i.e. the fluid in which the droplets are suspended. The third inlet port will be for the dispersed flow fluid, i.e. the fluid that will be made into droplets. Both continuous fluid and droplets suspended in that fluid will move to the outlet port and out of the device. The number of inlet and outlet ports for this device were chosen to make the usage of the device as simple as possible.

4.4 PDMS Pumps

The PDMS pumps are used to show how fluids can be manually mixed on the micro level without the use of electric pumps.

4.4.1 Durable

The durability is important for this device. Tests were performed to determine if two, three, or four coats of PDMS should be applied to the pumps. It was determined that three and four coats worked about the same, and both were better than two coats. To keep cost low application of three coats of PDMS applied to the sponges during fabrication gives the best durability.

4.5 Gradient Mixer

The gradient mixing device is intended to show both laminar flow and mixing at the microscale, and the ability to manipulate flows through the use of unique geometries.

4.5.1 Number of inlet ports

This specification supports the customer need of demonstrating microfluidic scaling laws.
The final gradient mixer device will be broken into two portions: a laminar flow portion and a gradient mixing portion. The laminar flow portion will include three inlets. These three fluids will flow in a channel together and ultimately combine into internal inlet ports to the gradient mixing portion. The gradient mixing portion of the device will include two inlet ports. See Fig. 9.2.5 located in Appendix 9.3 for clarification on the locations and types of inlets.

4.5.2 Flow rate of all fluids

This specification supports the customer need of demonstrating microfluidic scaling laws.
As stated above, the final gradient mixer device consists of two portions. The three inlets to the laminar flow portion will be controlled by syringe pumps. Ideally, all three input fluids will flow with equal flow rates. This will ensure a smooth gradient of mixed fluids at the outlet. If these flows are not equal, the gradient may be shifted more heavily toward the fluid with the higher flow rate. In order to be more interactive, however, the middle inlet flow will likely be adjustable to demonstrate the ability to control the width of the fluid flows in the laminar region of the device. The syringe pumps that will be used have the capability to provide a variety of controlled flow rates, but a rate of 50 μL/min will provide a low Reynolds number as well as a low Peclet number, resulting in laminar flow and diffusion as the dominant mixing method. See Fig. 9.2.6 in Appendix 9.3 for clarification on the various inlet flow rates.

4.5.3 Effective mixing

This specification supports the customer needs of demonstrating microfluidic scaling laws and incorporating interesting design aspects. Since the purpose of this device is to output a gradient of mixed fluid, each output channel will not have the same percentage of mixing. However, the center channel should demonstrate equal, complete mixing of the fluids. Ideally, the percentages mixed should be distributed normally around the center channel. An array of measurements will be made in the center mixing channel with a microscope capable of measuring RGB values. To demonstrate equal mixing, color uniformity should be present can be quantified through percentage difference between RGB values throughout the channel.

4.6 PDMS Lens

The PDMS lens introduces the concept of micro-lenses, which have applications in cytometry and fluoroscopy, in an interactive way through acting as a tunable cell phone microscope lens.

4.6.1 Number of inlet ports

In order to manipulate the lens, fluid must be pumped into the channel. This requires at least one inlet, but two inlets are desired in order to allow for easy removal of bubbles. This specification was determined through experimentation, during which bubbles in the lens were inhibiting the functionality of the device.

4.6.2 Membrane thickness

In order to better satisfy the customer requirement of durability while also providing enough elasticity to deflect and form the plano-convex lens, the thickness of the PDMS membrane should be at least 100 µm thick. During prototyping, this thickness was determined to be durable enough to withstand countless inflations and deflations of the lens.

4.6.3 Radius of lens

The smallest radius that is possible for the lens to achieve is limited by the radius of the channel. In order to achieve the greatest range of magnification possible, the channel should be chosen to be the smallest of the radii determined theoretically to produce such magnification. Through computer simulation, this minimum radius was determined to be 0.34 cm, as will be discussed in later sections.

4.6.4 Optical zoom

In order to provide a fun, interactive device for students, the lens should be capable of achieving a noticeable difference in magnification. The higher the magnification, the better. Optical zoom is determined by the maximum and minimum focal length. In this case, the maximum focal length is determined without the lens attached to the camera, and the minimum focal length is determined with the lens attached and deflected. This effectively provides the user with the specified optical zoom capabilities.

4.7 Hydrophobic PDMS Cubes

The hydrophobic PDMS cubes are meant to demonstrate how surface roughness affects the contact angle of droplet of water on a surface.

4.7.1 Surface roughness

Surface roughness greatly affects the contact angle of water on a hydrophobic surface (PDMS). The rougher the surface, a higher contact angle can be achieved. To achieve a rough surface without the aid of treating PDMS, granulated and powdered sugar, and a combination of both, will be placed on top of the sugar cube prior to PDMS soaking of the sugar cube, which relates to the customer specification of being demonstrable.

4.8 Micro Pin Valves

The micro pin valves are meant to demonstrate fluid-flow interactions and the relative turbulence of said fluids with no external power source or change in flow rates.

4.8.1 Number of inlet ports

The number of inlet ports should be maximized so that more colored fluids can flow through the channels. After considering the size constraints of the wafer used for making the molds and the amount of pumps available, the ideal number of inlet ports is three. Using the maximum number of colors will help further demonstrate the concepts integral to the micro pin valves.

4.8.2 Number of pin valves

To maximize the demonstrability of this device, the number of pin valves on the chip should be at least four pins per inlet. Due to size constraints, and after choosing three inlet holes, 12 pins will be incorporated on this chip to maximize the amount of interaction users can have with this chip.

4.8.3 Number of channels per inlet

Similar to the number of pin valves, there will be four channels of varying widths per outlet. This specification was chosen in tandem with the previously determined specifications, and in order to maximize demonstrability of the device and so the user can have more variety in dictating fluid flow.

4.8.4 Channel width

This specification does not necessarily have an ideal value; rather, it has an array of values that can demonstrate changes in fluid flow. Four channels widths were determined – based on a Reynolds number analysis – that would best characterize changes in fluid flow in relation to each other regarding their relative turbulent flows.

4.8.5 Block or allow fluid flow

This specification relates to the PDMS pins that are pushed down to block fluid flow or pulled up to allow flow. This is a binary specification in that the pins will either successfully allow for either blocking or allowing fluid flow that relates to the specification of being interactive.

4.9 Capillary Action

The capillary action device demonstrates how the effect of capillary action is more apparent in sufficiently small micro-channels and that the heights to which fluid can rise is dependent on the width of channels.

4.9.1 Number of inlet ports

Ideally, the number of inlets should only need to be one port that the user can replenish with fluid to allow for easy operation of the device. The single inlet can split into multiple directions to reach their respective channels. There needs to be at least one outlet, but unlike the other devices, this outlet serves only to remove the air in the channel as it is being filled with fluid; capillary action stops once the forces are balanced by the weight of the fluid.

4.9.2 Channel width

The widths of the channels in the device is critically important in the demonstration of the capillary action microfluidic phenomena. The maximum height to which fluid can rise up a channel against gravity is, to a good approximation, inversely proportional to the channel width. The device will feature channels ranging from 100 – 1500 μm in width. There is no ideal width in the channels since all widths will exhibit the capillary action phenomena.

4.9.3 Fluid type

PDMS is highly hydrophobic under normal conditions. Therefore, there is little to no adhesive interaction of water molecules to the surfaces of PDMS. Since adhesion is a critical contributor to the capillary action phenomenon, water cannot be used as a fluid and needed to be replaced with isopropyl alcohol. Although isopropyl alcohol (rubbing alcohol) does not meet the ideal NFPA rating of 0 as a completely non-hazardous fluid, it is still a widely available in most first aid kits as a standard antiseptic and is safe under normal conditions with proper handling.

4.10 Electrowetting

This device demonstrates the principle of electrowetting-on-dielectric, which is the ability of a surface that is typically hydrophobic to water to become more hydrophilic by an applied electric field. By using the phenomenon of electrowetting, the contact angle and even displacement of a water droplet can be controlled.

4.10.1 Fluid type

The electrowetting device should function for any water including tap water. However, if a droplet were to be left to dry, it would leave water marks due to impurities which can ultimately affect the hydrophobicity and performance of the device. For this reason, only ultra-pure deionized water will be used. Ions in the water are not necessary because the droplet itself does not need to be electrically conductive.

4.10.2 Electrode size

The size of the electrodes needs to be small enough to minimize the required droplet size while still being large enough so that applying the appropriate droplet size is not difficult nor require a microscope to operate.

4.10.3 Activation voltage

The electrostatic force that moves the droplet is proportional to the square of the applied voltage. Increasing the voltage will increase the allowable droplet size and the speed it moves to the next electrode. Either the dielectric breakdown voltage or the droplet saturation voltage, whichever is lower, limits this specification.

4.10.4 Droplet size

Directly related to this specification is the electrode size. Ideally, the droplet needs to be slightly larger than the electrode upon which it sits. This allows the droplet to fully cover an electrode while also being in contact with the neighboring electrodes, which is a requirement for the droplet to move.

4.10.5 Durable

The device is not necessarily easy to manufacture relative to the other LOC devices due to the many processing steps but they are easy and cheap to replace since they are fabricated in batches. The durability of the device refers to the Parylene that serves as both the dielectric and hydrophobic layers.

5. Design Development

5.1 Benchmarking

Benchmarking was done for the device-set as a whole, not for individual chip functions. Therefore, the metrics below are applicable for all devices. No microfluidic teaching pre-packaged sets were found, so comparisons were made to general microfluidic fabrication companies and experiments.

Table 5.1.1. Benchmarking data.

Metric #	Need #	Metric	Importance	Unit	Microfluidic LOCS (our devices)	Microfluidic Chip Shop Straight Channel Chips	Microflexis Standard Microfluidic Chips	ThinXXS Microfluidics Snake Mixer Slide	Journal of Chemical Education Experiment
7	6	Channel width	5	µm	20 – 100	20 – 1000	200	50 – 500	>50
7	6	Channel depth	5	µm	20 – 200	20 – 200	50	50 – 500	50 – 500
8	8	Low cost	4	$	30 – 50	41.1 – 48.26	N/A	61	20

5.2 Device Fabrication

5.2.1 Wafer and PDMS Fabrication

For a majority of the devices, the following steps were taken to fabricate the LOCs; the sugar cubes and electrowetting devices use different fabrication methods and are discussed in the latter two parts of this section.

Conceptual 2D AutoCAD drawings are the first step in creating a device. The drawings are used to produce a photomask that is transparent in areas where channels exist and opaque elsewhere. SU-8 is a chemically amplified, epoxy-based negative photoresist widely used in micro-devices to place thick-film channels on a silicon wafer. The process begins by spin coating a film of SU-8, the thickness of which is determined by RPM, RPM/s, and spin time. Next, the wafer is soft baked on a hotplate to evaporate the solvent in the photoresist that makes it liquid. After the soft bake, the wafer is exposed using a mask aligner with a UV lamp, using the aforementioned photomask as the pattern. A UV lamp, with a wavelength ideally around 350-400 nm and a dose of 600 mJ/cm^2, allows for the pattern on the mask to be transferred to the wafer. A post-exposure bake is then performed to harden the exposed portions of the film. Next, the SU-8 is developed with a chemical developer to remove unexposed areas off the wafer. Finally, the wafer is rinsed and dried and is ready to be used as a master for device procurement using PDMS.

Polydimethylsiloxane (PDMS) is a silicon-based polymer that is used in many microfluidic devices. To create PDMS, a base elastomer and curing agent is mixed in a 10:1 ratio and placed in a vacuum to degas. Next, the PDMS is poured over a SU-8 master in a container, such as a petri dish, and allowed to cure for either 48 hours at room temperature or 4 hours in an oven at 65°C. After full curing, the PDMS molds are removed from the wafer and inlet holes are created using biopsy punches. The channels are sealed to a substrate, which can be a glass slide or another piece of PDMS, using corona bonding (plasma surface activation). With the channels bonded, the device can now be used for the desired microfluidic application.

5.2.2 PDMS Cubes & Pump Fabrication

The fabrication of the PDMS cubes and pumps starts with a simple sugar cube. The sugar cube is placed in a glass petri-dish with a small amount of uncured PDMS. The petri-dish is placed in a vacuum for approximately three hours. This allows the PDMS, by capillary action, to fill in all the spaces between the individual sugar granules. Then, the oven is turned on to 180°C to cure the PDMS for about twenty minutes. This is the final step for the PDMS cubes; to produce pumps, the sugar is then dissolved from the cured PDMS filled sugar cubes by soaking them in warm water while simultaneously squeezing the cubes leaving only the PDMS sponge behind. Then, the PDMS sponges are coated with PDMS and cured to seal all the edges of the sponge. Finally, holes are made with a biopsy punch, one in the top and one in the bottom of the pump. The hole on top is for pressure release while pumping, and the hole on the bottom is to allow the pressure from the pump to move the fluid through the channels.

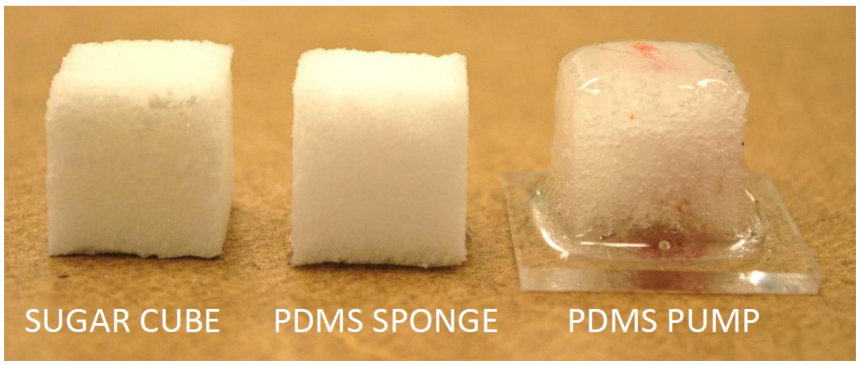

Figure 5.2.1. Picture during fabrication from sugar cube to pump.

5.2.3 Electrowetting Fabrication

The electrowetting devices are fabricated on standard 3”x1” glass slide substrates. The substrates are blown with a nitrogen gas gun frequently between every step to remove any stray particles. The glass slides are initially cleaned and prepared using buffered oxide etch and oxygen plasma treatment to provide an immaculately clean surface.

A 100 nm layer of chromium metal is deposited on one side of the glass slides using electron-beam physical vapor deposition. The electrodes are formed using standard photolithography techniques with a positive photoresist (S1813) while areas unprotected by photoresist are etched away by a chrome etchant.

The next step is to deposit 1200 nm of Parylene C (hereby referred to as just Parylene) that serves as both a dielectric insulator and hydrophobic layer using a Parylene coater.

Formation of the hair-thin (50 μm wide) grounding lines that span across the two rows of electrodes is done using a lift-off photoresist (NLOF 2020). The photoresist will protect any areas not to be deposited. A 50 nm layer of chromium is deposited using the same method as the electrodes. The lift-off is then removed using an ultrasonic bath of heated developer, leaving only the ground lines. The devices are rinsed with acetone and IPA then dried using nitrogen gas.

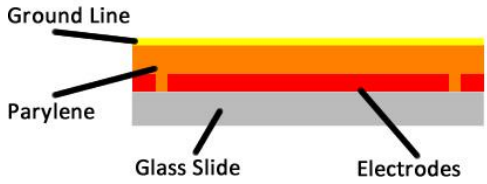

Figure 5.2.2. Diagram of electrowetting device depicting the electrode and Parylene layers built on a glass slide substrate.

5.3 Micro-droplet Formation

5.3.1 CFP Motivation

A CFP is generally not an entire device, but for the micro-droplet formation device the CFP is the formation of micro-droplets. This device is wholly based on showing the formation of micro droplets and to relate real world applications to students.

5.3.2 CFP Conceptual Design

The CFP design used was a cross-flow geometry (Fig. 5.3.1). The device was tested using varying flow rates of the dispersed and continuous flow fluids to create a continuous flow of micro-droplets through the channels. The droplets were measured to determine droplet volume using Eq. 1 in section 5.3.3 below. Obtaining a steady droplet volume is how the CFP requirement of continuous droplet formation was quantified. A range of flow rates was used to determine the best ratio of flow rates. An overview of how the flow rates were applied is listed below, but does not encompass all rate tested.

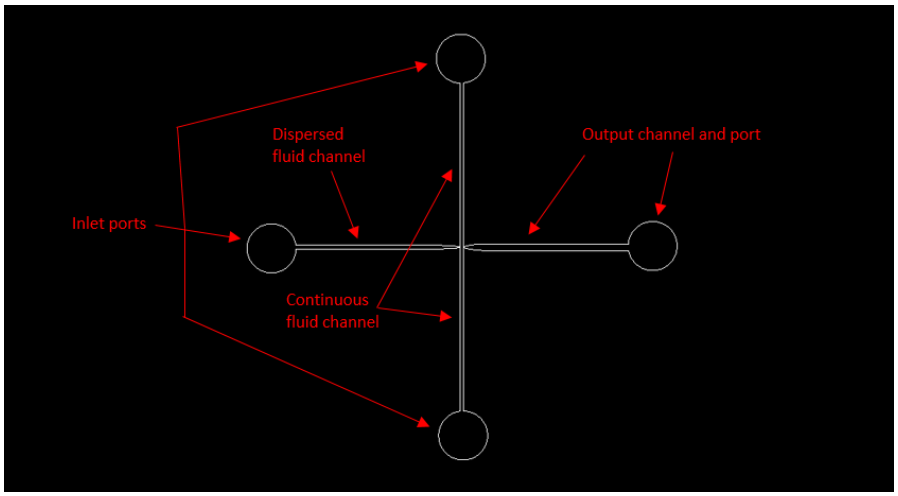

Figure 5.3.1. Conceptual design for droplet device

Table 5.3.1. Partial list of device parameters for CFP testing.

	W_c (µm)	W_d (µm)	Flow Rates (continuous:dispersed) (µL/hr)
Device 1	100	50	2:1
Device 2	200	200	1:1
Device 3	400	600	.8:1
Device 4	600	1000	.6:1

5.3.3 Theoretical Analysis and Calculations

The following formula was used to determine droplet volume once continuous droplets are being formed. The variables a and b are correction factors that will be determined at a later time if needed. W_c and W_d are the widths of the continuous and dispersed fluid channels, respectively. Q_d and Q_c are the flow rates used for the dispersed and continuous fluids through the channels, respectively.

$$V_d = aW_cA_d + bW_dA_c\frac{Q_d}{Q_c} \quad (1)$$

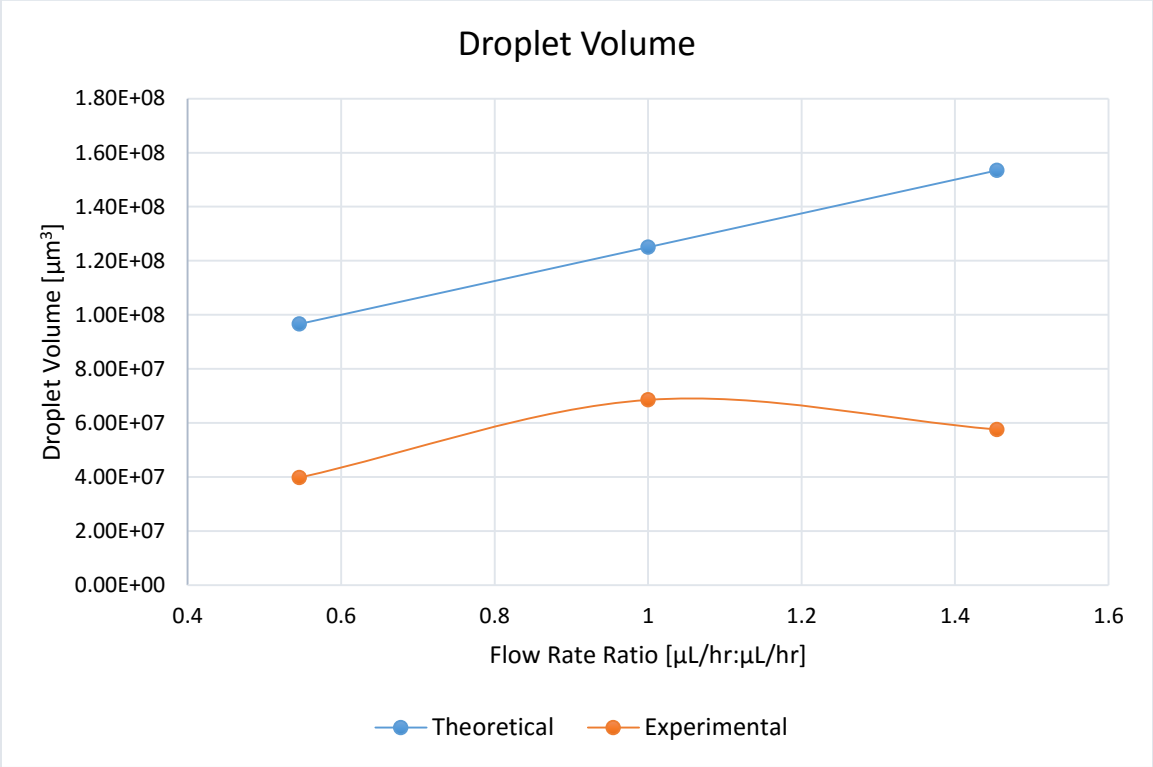

Figure 5.3.2. Plot of Theoretical droplet vs experimental volume with increasing flow rate ratio.

5.3.4 Testing Procedure

The device was tested using dyed water as the dispersed flow fluid and olive oil as the continuous flow fluid. Different flow rate ratios were used starting with the rates listed in Table 5.3.1. These rates were adjusted up or down to try to achieve droplet formation with this particular geometry. Using adjustable pumps to control the flow rates and a microscope to view the device in action more closely, the flow rates were adjusted depending on how the fluid flow was moving through the channels.

5.3.5 Experimental Test Results

After many failed attempts with the initial device geometry (T-junction, Appendix 9.1, Fig. 9.1.1), the geometry was changed to a cross-flow design. Using the new design, micro-droplets were successfully formed. The device was put under our microscope where pictures and measurements of the droplet diameter were captured which can be seen in Fig. 5.3.2. The measurements were used to determine the experimental droplet volume based on flow rate. These results are compared to the theoretical values shown in the graph above.

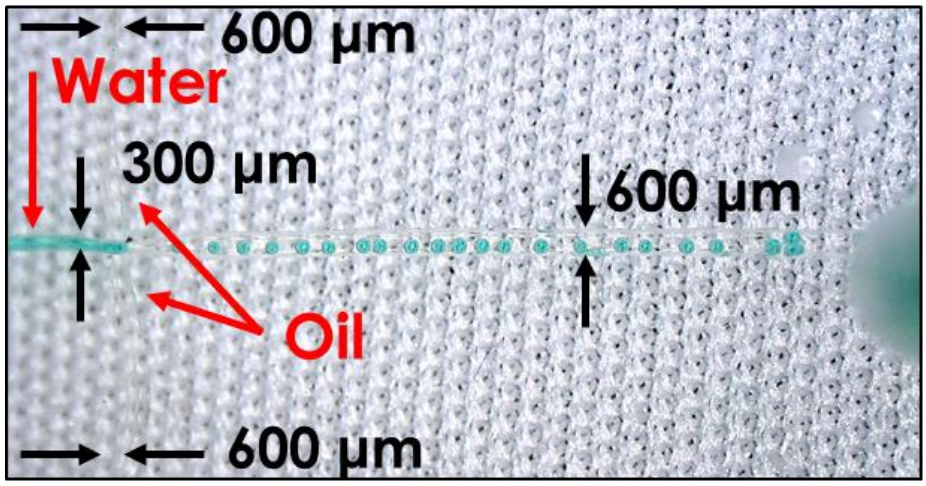

Figure 5.3.3. Micro droplet formation showing device geometry.

Referring back to Table 4.1 in the design specification section, the micro droplet device meets all of the applicable specifications. This device is interactive, durable, and shows a particular micro phenomenon that can be linked directly to real-world application. This device is inexpensive to fabricate, and has a power point presentation that can be used in lecture before a lab demonstration of the device.

5.3.6 Final Design and Future Revision

The final design will not change. I was able to use the new geometry design to form micro droplets and with the end of the project near there will not be time to make any more revisions or do any more testing.

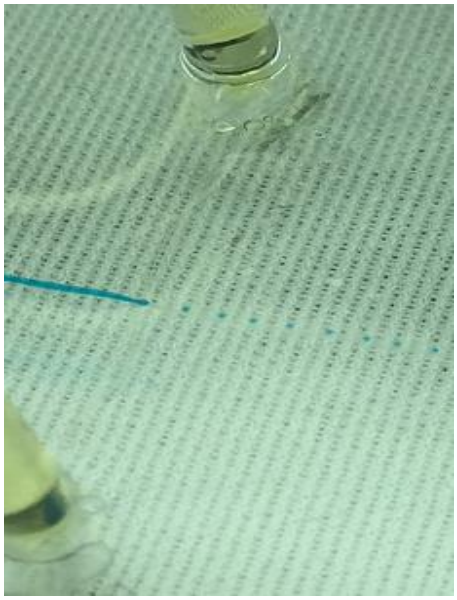

Figure 5.3.4. Final micro device design.

5.4 PDMS Pumps

5.4.1 CFP Motivation

The CFP for this device is having a durable PDMS pump with the ability to manually push fluids through a gradient mixer.

5.4.2 CFP Conceptual Design

Only one way to fabricate the pumps will be used; however, the number of final coats of PDMS applied to the pumps will need to be determined. To verify a pump to meet the CFP specifications, pumps with two, three, and four coats will be compared to determine pumping efficacy and durability.

5.4.3 Testing Procedure

Testing on the PDMS pumps was performed to determine the effectiveness of the pumps to move fluid through a gradient mixer, and the overall durability of the pumps. Four pumps were fabricated, using two, three, and four coats of PDMS to be compared for testing. The pumps were used to pump blue and red dye through a gradient mixer, and red-blue (RB) light intensity values were measured using Photoshop at the gradient mixer outlet for pumps of each coating thickness. These RB values were then compared to the RB intensity values of a 50/50 mix of red and blue dye from the same batch of fluids. The durability was determined by pushing the pumps to 100 pushes or until failure.

5.4.4 Experimental Test Results

Test results from comparing RB intensity values for individually pumping red and blue through the gradient mixer and pumping the 50/50 mix were nearly identical. The durability test results show that pumps with only two coats are the least durable and none of them lasted to one hundred pushes. The three and four coat pumps lasted to one hundred pushes, but some lasted less than twenty pushes. This shows that the fabrication methods available are not consistent, but that the three and four coat pumps are more durable. Considering three and four coat pumps are similar in durability and pumping effectiveness the three coat pumps were selected as the best choice based upon the project specifications. The results are listed below in Table 5.4.1.

Table 5.4.1. Experimental test results for PDMS pumps.

	Average RB values at exit	% difference from 50/50	Pumps failed before 20 pushes	Pumps that reached 100 pushes
2 coats	92.55	10.5	All	-
3 coats	102.35	0.43	1	3
4 coats	95.5	7.36	2	2
50/50 mix	102.8	-	-	-

Referring back to Table 4.1 in the design specification section, the PDMS pumps meet all of the applicable specifications. This device is interactive, durable, and demonstrates a link directly to real-world application. This device is inexpensive to fabricate, and has a power point presentation that can be used in lecture before a lab demonstration of the device.

5.4.5 Final Design and Future Revision

The design is not going to change and there will be no future revisions now that the best choice for number of coats has been decided.

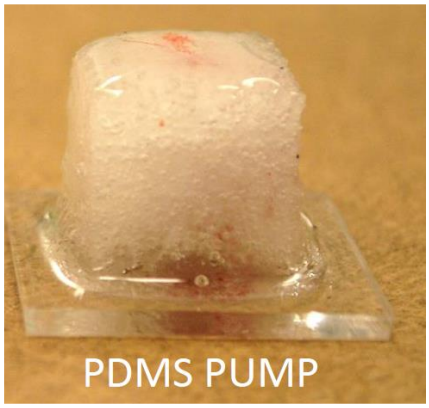

Figure 5.4.1. Final PDMS pump design.

5.5 Gradient Mixer

5.5.1 Brainstorming

There are many ways to induce mixing in microfluidic channels through the manipulation of channel geometry. Some examples include serpentine channels, Dean flow mixers, obstructions in channel, and extrusions in channel walls, among others (Appendix 9.2, Fig. 9.2.1). While considering the customer needs of cost and unique designs, a design matrix (Appendix 9.2 Table 9.2.1) was created to rank possible configurations.

5.5.2 CFP Motivation

The purpose of this CFP was to determine which channel geometry would provide the most complete mixing in the gradient mixing device. Four channel geometries were tested at five different flow rates. The five flow rates were 5, 10, 20, 50 and 200 µL/min. The purpose of the five flow rates was to determine the effect of flow rate on mixing through diffusion. Fig. 5.5.1 shows the chip that was fabricated using the SU-8 cleanroom fabrication method.

Complete mixing through the appropriate channels is required for the desired output of a smooth gradient of color. This relates to the customer needs of providing a unique and interesting design showing scaling phenomena and effective mixing. Due to the laminar flow of the fluids, mixing must be induced through channel geometry manipulation and through diffusion. Channels designed to disrupt streamlines of the laminar flow and create turbulence in the channel can promote mixing. Mixing through diffusion is maximized at low flow rates, described by the Peclet number.

The microscope that was used to observe this prototype had the capability to capture pictures. These pictures were analyzed using Photoshop and evaluating RGB values of pixels at the channel outlet. The uniformity of color at the channel outlet was determined (Appendix 9.2 Tables 9.2.2 – 9.2.6) and this value was used to determine the amount of mixing through the channel.

5.5.3 CFP Conceptual Design

Fig. 5.5.1 shows the DXF file used to create the gradient mixer CFP. Four different channel geometries were created: a square serpentine channel, a round serpentine channel, a vertical blockade channel, and horizontal blockade channel. All the channel inlets and outlets as well as the serpentine channels were designed to have channel widths of 100 µm. All four chips fit within a 3x1 inch glass slide.

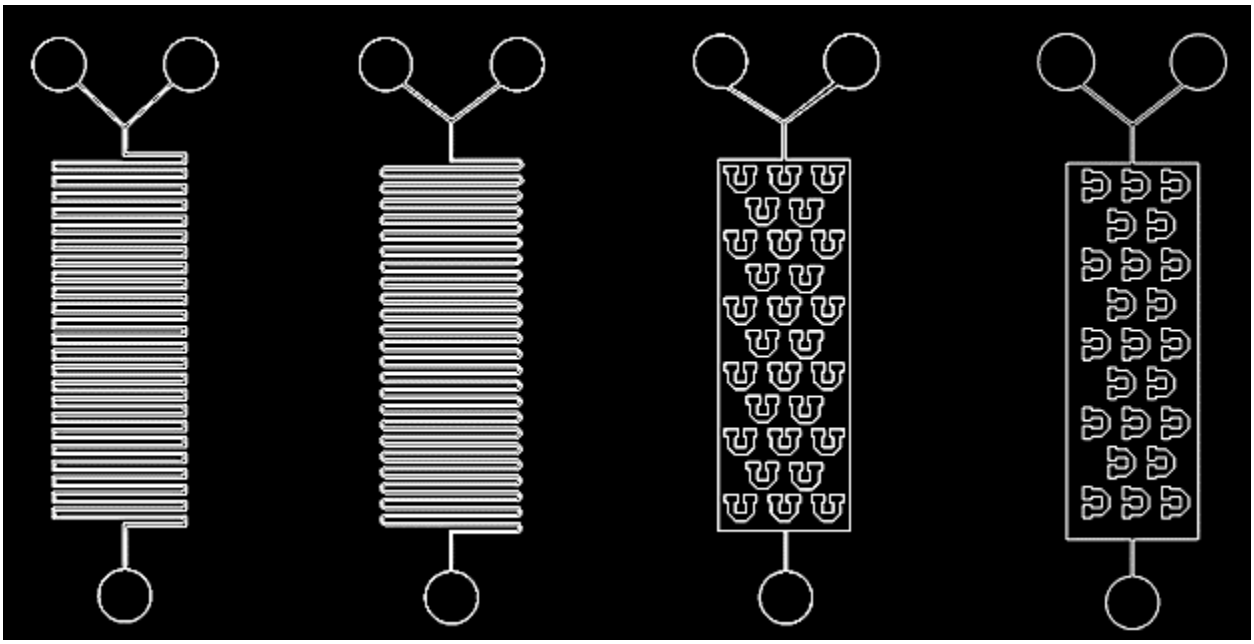

Figure 5.5.1. Gradient mixing CFP DXF file. From left to right: square serpentine channel, round serpentine channel, vertical blockade channel, horizontal blockade channel.

5.5.4 Theoretical Analysis and Calculations

Design of the gradient mixer was based primarily on two non-dimensional numbers - the Reynolds number and the Peclet number. The Reynolds number represents the ratio of inertial forces to viscous forces and is defined by the following equation where ρ is fluid density, v is fluid velocity, L is characteristic length, and µ is dynamic fluid viscosity.

$$Re = \frac{\rho v L}{\mu} \tag{2}$$

A low Reynolds number, specifically less than 2500, indicates that the flow is laminar. An analysis was performed using channel lengths between 10 and 2500 µm at a range of fluid flow rates from 5 to 200 µL/min, which are typical values in microfluidic systems, and it was found that the Reynolds number was much lower than 1, indicating that the flow is laminar in all cases (Fig. 5.5.2). Table 5.5.1 shows the fluid properties and dimensions used in the analysis.

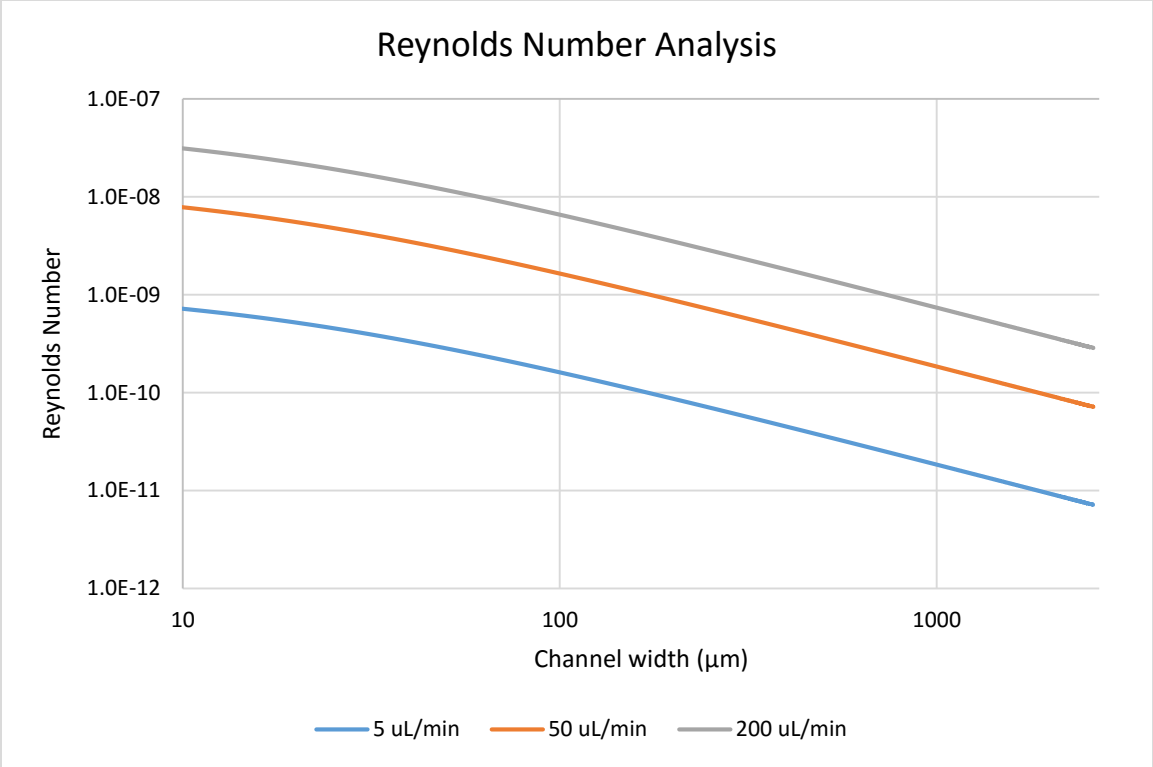

Figure 5.5.2. Reynolds number analysis for range of channel widths at three fluid flow rates. All values in these cases are much less than 1.

Table 5.5.1. Property table for Reynolds number analysis.

Property	Value	Unit
Density	1000	kg/m^3
Dynamic Viscosity	0.89	mPa·s
Depth of Channel	120	µm

The Peclet number is a dimensionless number that describes the ratio of the advection transport rate to the diffusive transport rate. The following equation describes the Peclet number where L is the characteristic length, v is the velocity, and D is the mass diffusion coefficient.

$$Pe = \frac{Lv}{D} \tag{3}$$

When Peclet number is low, below 1, diffusion is the primary mode of mixing. An identical analysis to the previous Reynolds number analysis was completed and it was found that all expected Peclet numbers were well below 1 (Fig. 5.5.3). This result indicates that diffusive mixing is expected to be the prominent form of mixing through the channels. In this analysis, a diffusion coefficient of 2.3E-9 m^2/s was assumed.

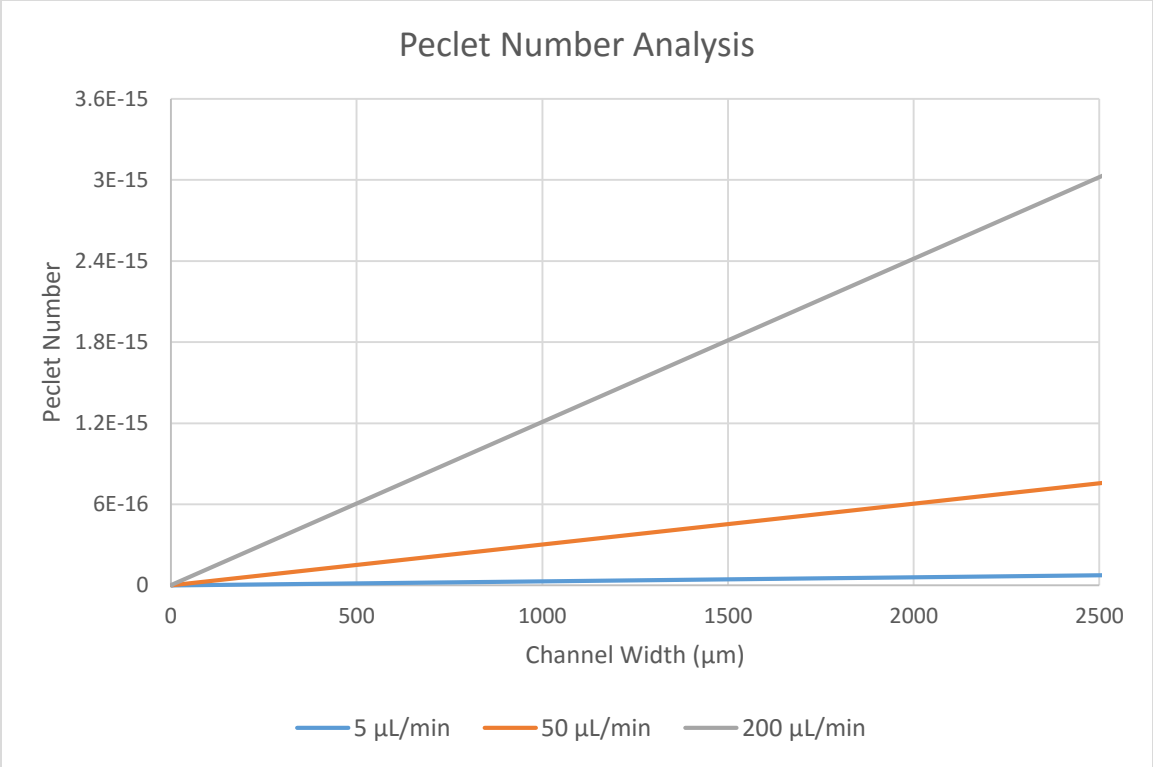

Figure 5.5.3. Peclet number analysis for range of channel widths at three fluid flow rates. All values in these cases are much less than 1.

5.5.5 Testing Procedure

The gradient mixer CFP chip was produced using two different fabrication methods. The first iteration was fabricated using laser-cut tape and PDMS. This method was not suitable for the desired channel dimensions as many of the mold channels were damaged either by the laser or through the transfer process to a petri dish. Since this method did not produce sufficient results due to incomplete channel formation, another chip was fabricated using traditional cleanroom methods and SU-8 as described in section 5.2.1.

The completed CFP channels were tested using the Keyence VHX-5000 Digital Microscope, a syringe pump, and two fluids consisting of water and different colors of food coloring. Five flow rates were tested: 5, 10, 20, 50, and 200 µL/min. The two fluids were controlled by the syringe pump, and they both flowed at the same rate. Color photos of the entire channels were taken once the flow had reached a steady state. These color photos were then analyzed using Photoshop and the RGB values of pixels at the end of each channel. Ultimately, the uniformity of color at the end of the channel was used to determine whether sufficient mixing had occurred through the channel (Appendix 9.2 Tables 9.2.2-9.2.6)

5.5.6 Experimental Test Results

Table 5.5.2 shows the percent difference from typical uniform color of each channel for each flow rate. More information on this analysis can be found in Appendix 9.2.

Table 5.5.2. Color uniformity experimental results.

Flow Rate (µL/min)	Vertical Blockade	Horizontal Blockade	Rounded Serpentine	Square Serpentine
5	268%	212%	8%	58%
10	279%	302%	22%	24%
20	312%	336%	35%	43%
50	284%	292%	13%	30%
200	289%	218%	43%	5%

In Table 5.5.2, a smaller number represents more complete mixing, since it shows the percent difference from a typical uniform color. The uniform colors that the analysis was compared to were the red and blue inlet channels.

Fig. 5.5.4 shows an enlarged image of the rounded serpentine channel at a flow rate of 5 µL/min. Additional images of the CFP channels in action can be found in Appendix 9.2.

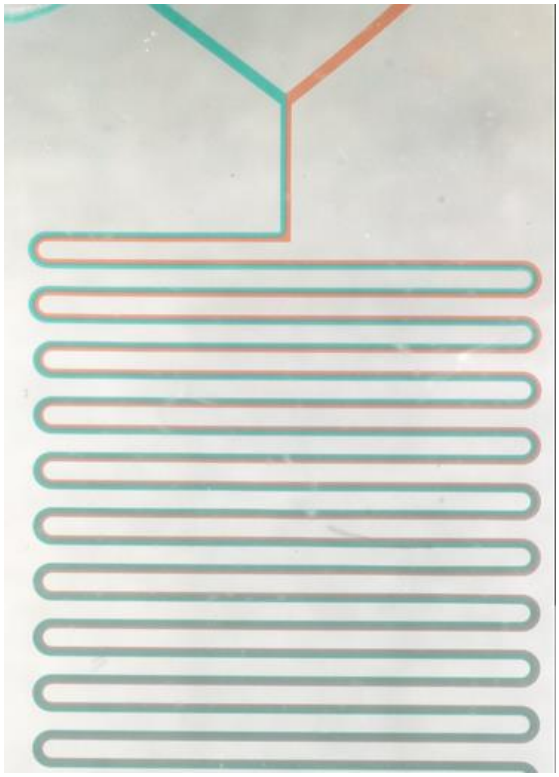

Figure 5.5.4. Top portion of rounded serpentine channel at 5 µL/min.

5.5.7 Final Design and Future Revision

The final gradient mixing chip consists of two portions: a laminar splitting portion and a gradient mixing portion. The gradient mixing portion will induce mixing through series of rounded serpentine channels. Fig. 5.5.5 shows a DXF file of the final design. The SU-8 fabrication method was used for this chip due to the small channel widths of 100 µm. Unfortunately, there were complications with the SU-8 fabrication, and ultimately a scaled-up, laser-cut version was created for demonstration purposes. The smallest dimensions on the scaled-up version was 500 µm, yet it still passed three different fluids through a series of 14 serpentine channels and fulfilled all customer requirements.

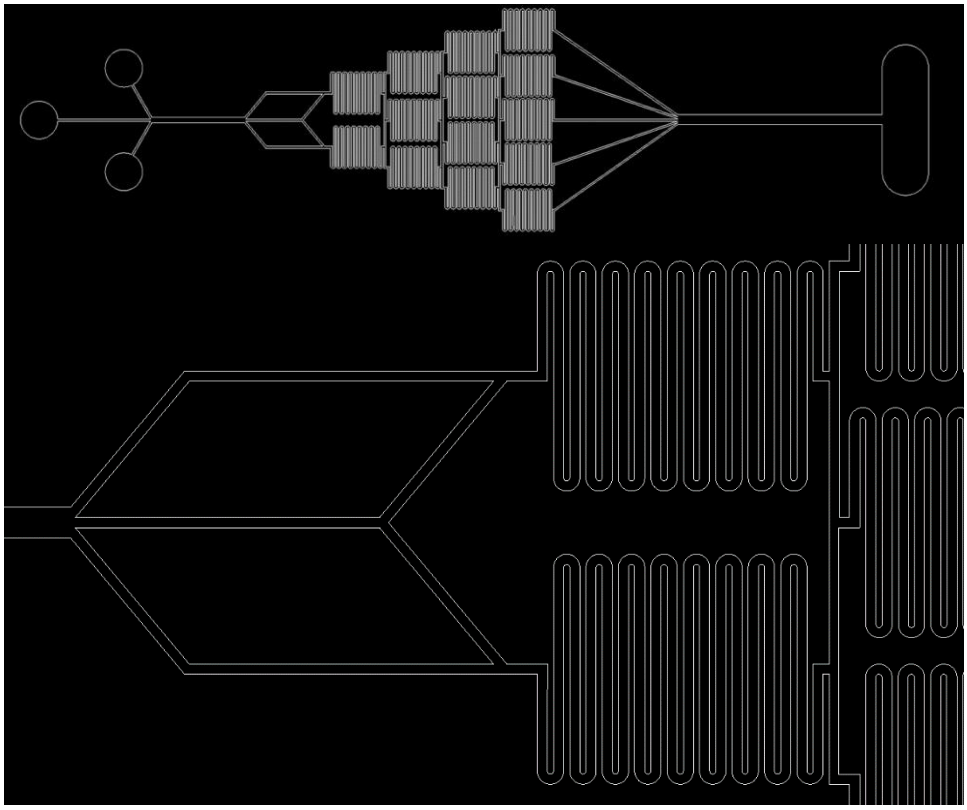

Figure 5.5.5. DXF file of final design with enlarged view of rounded serpentine channels

The following images show the final row of serpentine channels on the 500 µm thick mixer. This mixer was tested using two fluids, rather than three, in order to be comparable to CFP testing results of color uniformity.

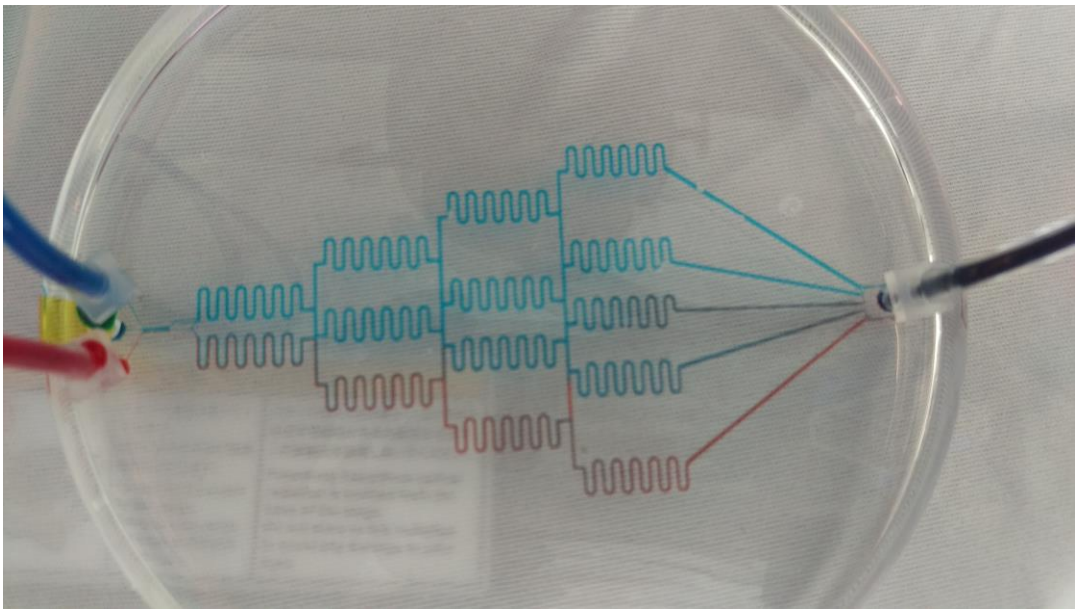

Figure 5.5.6. Final gradient mixing system.

While it is clear that the uniformity of color is not as good as the CFP rounded serpentine channels, overall the device still demonstrates gradient mixing well enough for the purposes of a lab demonstration. Ideally, the center serpentine channel on the final row, containing five serpentine channels, would have one uniform color. Calculations identical to those done in the CFP analysis showed a percent variance of 56.8% (see Appendix 9.2 Table 9.2.7), comparable to but worse than the results for the serpentine channels. This version of the mixer was deemed successful since it was still able to demonstrate both laminar flow and micro-mixing, in an interactive way, using colorful fluids. Ultimately, it still satisfied all the customer requirements addressed in Table 4.1, while failing on the mixing specification from Table 4.4.

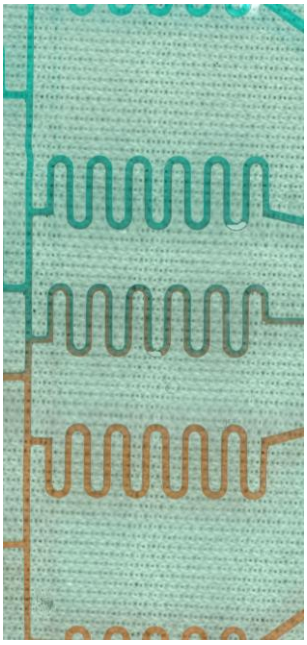

Figure 5.5.7. Final row of serpentine channels on 500 µm wide device.

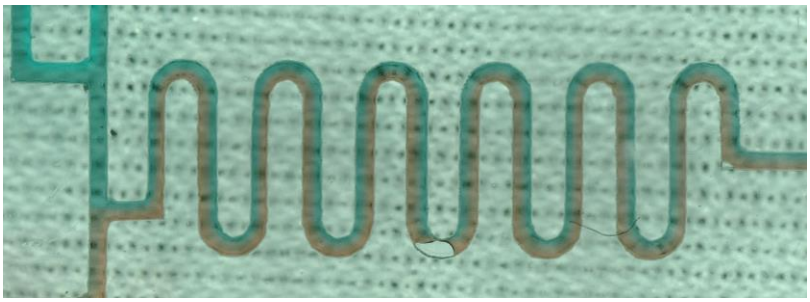

Figure 5.5.8. Closer view of middle serpentine channel shown in Fig. 5.5.7. It is clear that the red and blue channels do not fully mix by the end of the serpentine section.

Future revisions of this device include altering the DXF file slightly to incorporate a larger spacing between the serpentine channels. If the final fabricated device had been the 100 µm thick channel design, it is believed that better mixing would be achieved since this geometry would better match the successful CFP geometries. This is mainly due to the increased length of the channels, and the number of turns in the channel being 17 rather than 11.

5.6 PDMS Lens

5.6.1 CFP Motivation

There were a couple ways to fabricate a microfluidic lens. First, a large drop of SU-8 could have been cured and acted as lens. Second, the same SU-8 drop could have been used as a mold in which PDMS would be poured over. Third, a channel could be formed and molded with PDMS, and then bonded to a thin PDMS membrane. The last possible solution that was considered was a two-sided lens that could extend out in both directions forming a convex-convex lens. In the end, the third option was chosen because of its easy fabrication and the level of interaction possible.

There were multiple motivations behind this CFP. First, it was necessary to test if the fabrication method would work. During the Fall semester, it was discovered that the fabrication of the device was often much harder than expected. For the fabrication of the PDMS lens, the plan was to fully cure the piece of PDMS molded to the channel, and then apply the fully cured channel to the partially cured membrane.

Secondly, this CFP was used to verify to geometric concepts of the lens device. One, if the channel widths leading up to the lens chamber made a difference on the ease of filling the channel with fluid, and two, if there was a correlation between possible lens radii and the dimensions of the molded channel.

5.6.2 CFP Conceptual Design

The original CFP design consisted of one channel leading to the lens well, with a diameter of half an inch shown in Fig. 5.6.1. This diameter was chosen since it would fit over most cell phone cameras with ease. The widths of the channels increased from 50 to 500 μm.

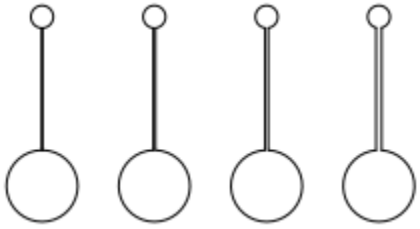

Figure 5.6.1. Initial prototype of lens.

The initial prototype was tested under a microscope to determine the correlation between molded channel dimensions and the minimum dimensions of the lens. It was determined that the minimum lens radius is limited by the channel dimensions – the lens can only be as small as the molded channel. This is because the lens experiences great elasticity as it is deforming and deflects as a perfect hemisphere, shown in Fig. 5.6.2. The widths of the channels did not have a noticeable effect on the difficulty of filling the lens with fluid.

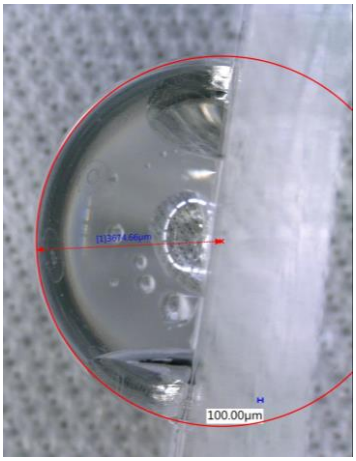

Figure 5.6.2. Lens deflecting in a hemisphere shape, limited by the half-inch diameter of the lens channel.

The second iteration of the prototype incorporated two inlets. As seen in Fig. 5.6.2, the initial prototype did not allow bubbles to be removed from the lens, which would ultimately ruin the ability of the lens to be used to magnify cell phone cameras. The process of eliminating bubbles in the second iteration involves first filling the channel with fluid while holding a finger over one inlet, with the other inlet connected to a syringe, then simultaneously removing the finger while physically pressing the air from the lens. After pressing the air from the lens, while still connected to the syringe, the inlet that was originally plugged by a finger can be blocked with a PDMS plug. Once plugged, the lens can be filled to the desired radius and then the syringe inlet can be blocked with the same type of PDMS plug.

Figure 5.6.3. Second prototype of lens.

The second iteration ultimately led to the final design, with a revision made to the size of the lens well to obtain the desired magnification, discussed in section 5.6.3. The channel widths leading to the well were kept at 500 µm to increase ease of fabrication using the laser cutter and vinyl tape.

5.6.3 Theoretical Analysis and Calculations

In order to determine the radius of lens that would provide the greatest magnification, numerical modeling on focal length and magnification was conducted. Both water and IPA were modeled as the lens fluid, since their respective indices of refraction of 1.33 and 1.37 are close to the index of refraction of PDMS, which is 1.4. Focal length was calculated using Eq. (4) where f is focal length, R is radius of lens, and n is index of refraction of the fluid.

$$f = \frac{R}{(1-n)} \tag{4}$$

Magnification was theoretically calculated using Eq. (5), where M is magnification, f is focal length, and p is the distance of the object from the lens.

$$M = \frac{-f}{(p-f)} \tag{5}$$

Table 5.6.1 shows the theoretical radii that would provide the maximum magnification for water. A negative magnification would indicate an inverted image, which was experimentally validated.

Table 5.6.1. Theoretical modeling results of lens radius and resulting magnification, using water as the fluid.

Lens Radius (cm)	Focal Length (cm)	Magnification 2.5 cm Away	Magnification 1 cm Away
0.34	1.02	-0.69	48.6
0.84	2.52	112	1.64
0.90	2.70	13.3	1.59

In addition to the numerical modeling seen above, a Matlab code (Appendix 9.3) was created to aid in the visualization of all the radii possible. This code provides a visual representation of the lens, and allows for the creation of physical inflation guides for the end user. By printing off figures similar to Fig. 5.6.4 below, one can visually match the radius of the lens to the desired size on the graph.

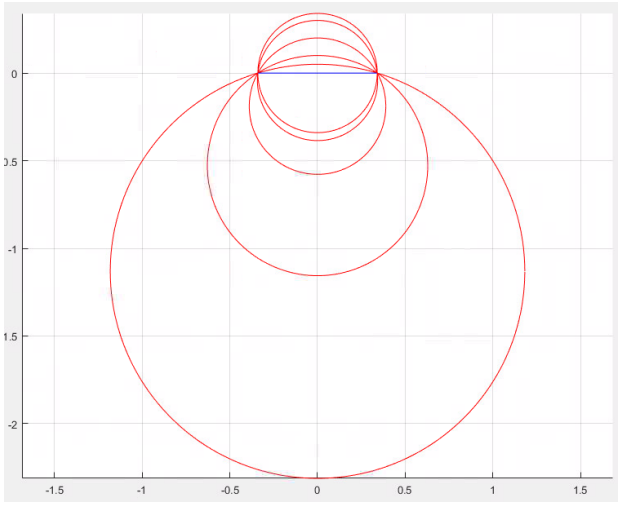

Figure 5.6.4. Matlab representation of possible lens radii, assuming 0.34 cm radius lens design.

5.6.4 Testing Procedure

The experimental setup for testing the functionality of the lens consisted of a mounted cell phone with a ruler secured perpendicular from the phone. A small printout of 8-point font containing the alphabet was used for the camera to focus on. First, the minimum and maximum focal lengths of the camera without the lens were measured, for a baseline. The lens was then filled up to two different radii, using a guide similar to Fig. 5.6.4, and the minimum possible focal length was measured.

These measurements were used to calculate optical zoom, which is more familiar to most end-users than magnification. Optical zoom is calculated using Eq. 6, using maximum and minimum focal lengths.

$$Z = \frac{f_{max}}{f_{min}} \tag{6}$$

5.6.5 Experimental Test Results

The experimental test results are show in Table 5.6.2. The maximum optical zoom measured was 37.3X, which is much greater than the required specification to be greater than 10X, and satisfies the ideal specification of being greater than 30X.

Table 5.6.2 PDMS experimental test results.

Parameter	No Lens	Small Radius Lens (0.34 cm)	Large Diameter Lens (0.84 cm)
f_{min} (cm)	20.5	1.00	2.50
f_{max} (cm)	55.9	55.9	55.9
Optical Zoom	2.72	37.3	22.4

Looking at the specifications Table 4.1 in the design specification section, the PDMS lens meets all of the applicable specifications, except for being able to withstand excessive handling. This device is interactive, uses non-hazardous fluids, accompanied by teaching material written in non-technical language, and is able to be set up within 15 minutes.

5.6.6 Final Design and Future Revision

The final lens design incorporated a lens with radius of 0.34 cm and two inlet ports. This lens satisfies all customer requirements except for the durability requirement. The lens is prone to popping, especially at the two inlets. It is a fragile device. An image of the final lens is shown in Fig. 5.6.5.

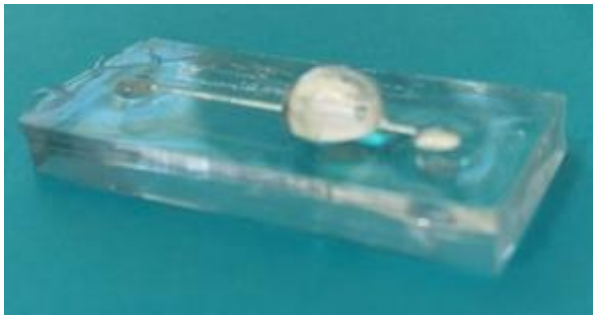

Figure 5.6.5. Final PDMS lens. Future revision would include a thicker membrane as an attempt to increase durability, and potentially bonding more PDMS over the inlet ports. Bonding more PDMS over the inlets would increase durability and make the device easier to setup, both of which would increase customer satisfaction.

5.7 Hydrophobic PDMS Cubes

5.7.1 CFP Motivation

This CFP, unlike most of the LOCs, is the device itself. The cube is designed to show how surface roughness affects the hydrophobicity and the contact angle of a droplet on a treated surface. Design motivations for this CFP involve using different methods of changing the surface roughness to show that the contact angle will increase.

5.7.2 CFP Conceptual Design

Five different surface-roughness-altering methods were conceptualized when designing for the cubes. The sugar cubes have highly alterable surfaces and will maintain whatever shape they are in before soaking up PDMS and being baked into solid cubes. Fig. 5.7.1 shows design sketches for ideas of altering the sugar cube's surface save the granulated/powdered sugar combination.

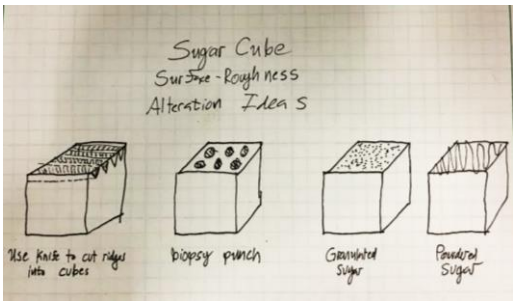

Figure 5.7.1. Conceptual sketches of four methods of altering surface roughness.

Five methods of changing the surface roughness were implemented: a knife-cutting method, which involved cutting horizontal and vertical lines across the surface of the cube in order to create a matrix on the surface; a circular punch method, which involves using a biopsy punch to dig holes into the surface; the third and fourth method involve placing powdered sugar or granulated sugar on the surface prior to PDMS treatment; and the fifth is a combination of granulated and powdered sugar. Fig. 5.7.2 shows each surface-altering method PDMS cubes. Another cube will be made that does not have its surface altered to show as a comparison to the altered surfaces.

Figure 5.7.2. Left to Right: matrix lines, biopsy punch, granulated, powdered, and combination.

5.7.3 Theoretical Analysis and Calculations

Wetting, which is a liquids capability of maintaining contact with a solid surface, measures the force between cohesive and adhesive forces. In order to increase wettability, the Wenzel contact angle model states that increasing surface roughness will increase the contact angle at which a liquid interacts with a solid surface. Eq. (7) shows the Wenzel model:

$$\cos(\theta^*) = r \cdot \cos(\theta) \tag{7}$$

Where θ^* is the apparent contact angle that is related to a stable, equilibrium state, r is the roughness ratio, which is apparent area of the surface over the actual area, and θ is the Young contact angle for an ideal surface - for PDMS, the Young's contact angle is 110°. Fig. 5.7.3 shows how when the surface roughness is increased, the contact angle also increases.

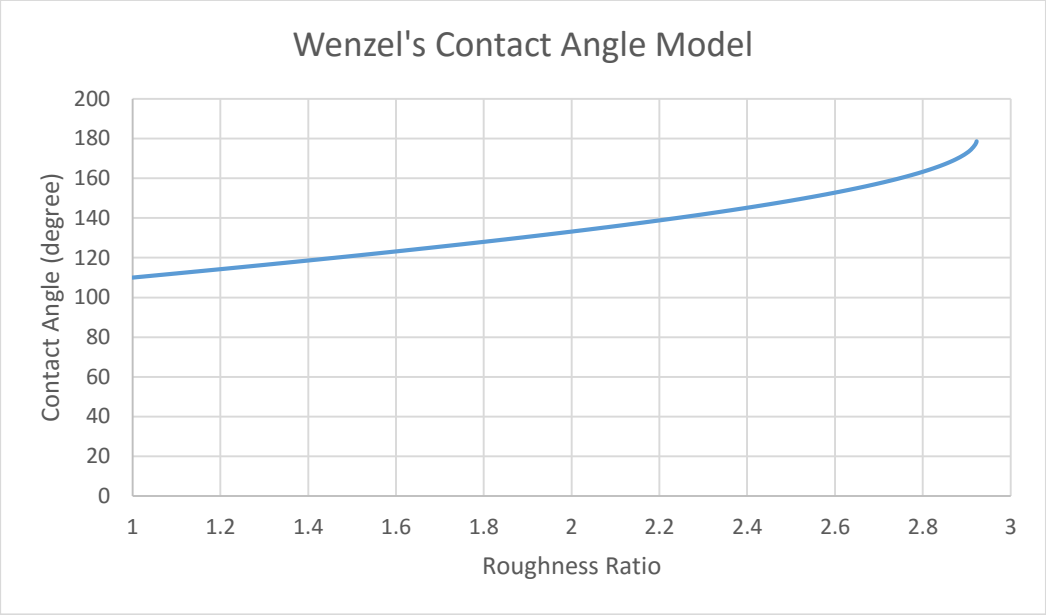

Figure 5.7.3. Relationship between the roughness ratio and the contact angle.

5.7.4 Testing Procedure

A droplet of colored water will be placed on top of the cube using a pipette. Once the droplet is on the cube, still shots will be taken with the Keyence VHX-5000 Digital Microscope to get a microscopic view of the liquid-surface interface. Using the Keyence microscope's built-in angle measuring tools, the contact angle of the droplets will be analyzed and documented.

5.7.5 Experimental Test Results

Fig. 5.7.4 shows Keyence microscope photos of the droplets on the different surfaces, and Table 5.7.1 shows tabulated data of the contact angle of the different surface-roughness altering methods, along with measurements of both untreated sugar cubes and untreated PDMS to show differences in contact angles

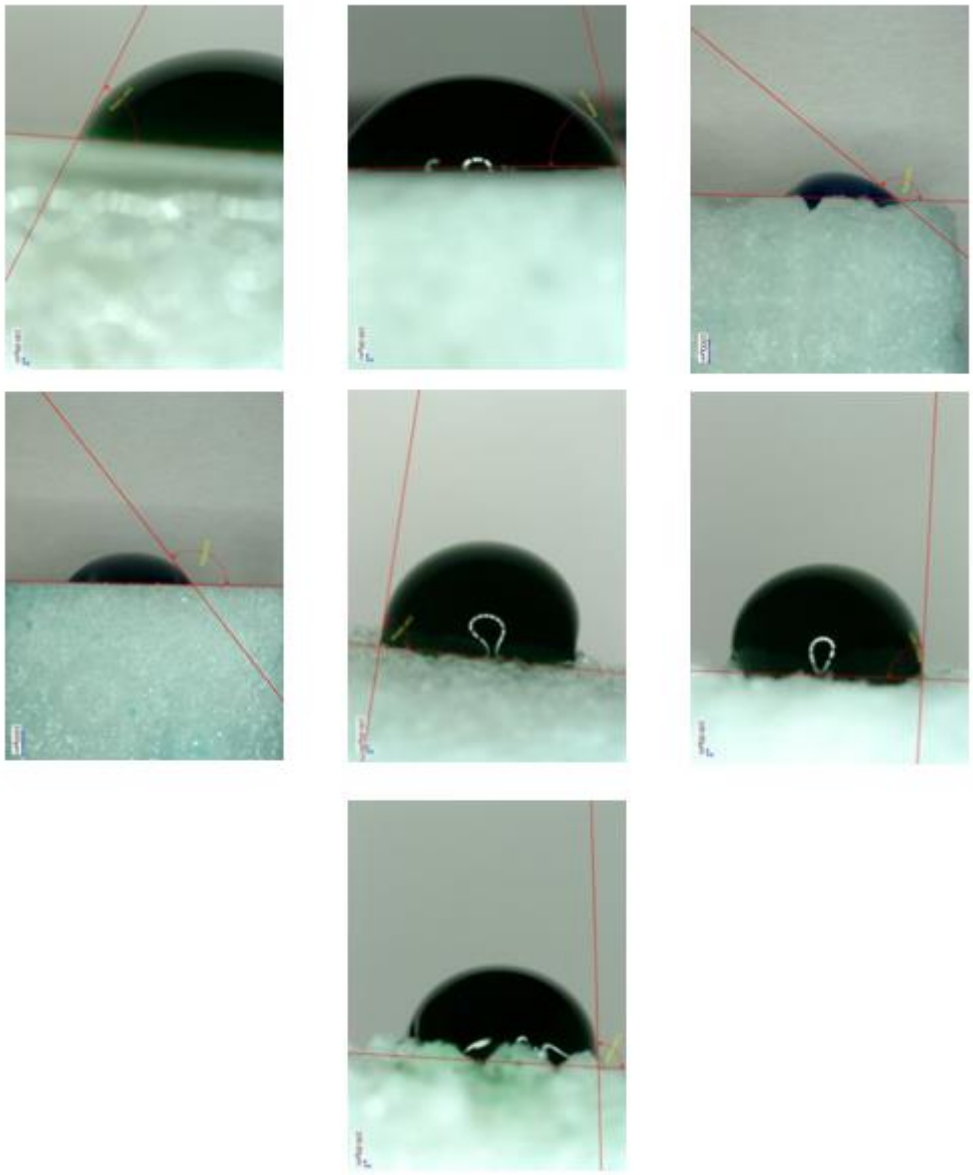

Figure 5.7.4. Top, left to right: flat PDMS surface, circle biopsy punch, matrix lines. Middle, left to right: Untreated sugar cube, granulated sugar, powdered sugar. Bottom: granulated and powdered sugar.

Table 5.7.1. Contact angles for each surface.

Roughness Treatment	Contact Angle (θ)
PDMS (no treatment)	67.33
Untreated sugar cube	77
Matrix cuts	40
Circular Punch	51
Granulated sugar	87.68
Powdered sugar	90.71
Granulated & powdered sugar	94.51

Based on the values in Table 5.7.1, surface treatment does affect the contact angle; however, both the matrix and circular punch treatments made the liquid-surface interface more hydrophilic, meaning the surface was more prone to holding onto water. These hydrophilic results can be explained by improper surface treatments, which will be explained in the following section. The granulated and powdered sugar, which have nano-sized grains, helped increase the roughness by about 27.18°.

Referring back to Table 4.1 in the design specification section, the cubes meet all of the applicable specifications. There are no inlets, outlets, and it is difficult to achieve unique geometries with a cube, but it meets the main specifications of being a safe, demonstrable, low cost, and easy-to-fabricate. The device demonstrates the appropriate scaling phenomena by user interactions, and is accompanied by an approved teaching module explaining hydrophobicity, equations used to model surface roughness, and real-world applications. The cubes can also withstand multiple tests, can be set up quickly, and are small enough to be packaged easily. The device also meets the device-specific specification of having its surface roughness altered.

5.7.6 Final Design and Future Revision

Due to the simplicity of the cubes, and after reviewing the results, no further design changes will occur. Three of the five surface-altering design configurations, shown in Fig. 5.7.5, are capable of creating more hydrophobic surfaces than their untreated counterparts, and the two that could not produce hydrophobic contact angles will not be used anymore.

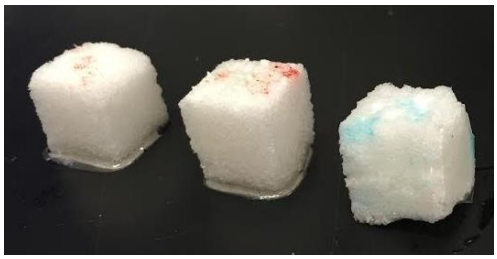

Figure 5.7.5. Granulated, powdered, and combination granulated/powder PDMS cubes.

For future surface treatment cubes, a more sophisticated surface-roughness treatment method would be used. For instance, a wafer could be manufactured to have channels as close as 10 μm apart, which could theoretically create a nano-surface-roughness structure capable of contact angles that are nearly superhydrophobic – contact angles over 150°. Other methods include chemical channel surface treatment that have low surface energies i.e. polytetrafluorethylene (PTFE).

5.8 Micro Pin Valves

5.8.1 CFP Motivation

The motivation behind this CFP was to test whether or not fluid-flow interactions could be controlled without the use of an external power source by using manually actuated pin valves to block or allow fluid to flow. Based on a Reynolds number analysis, as seen in a later section for this device, the relative turbulence of flow can be greatly changed by the fluid channel dimensions. Micro pin valves were fabricated to test the efficacy of blocking off channels.

5.8.2 CFP Conceptual Design

The design of the CFP, Fig. 5.8.1, consists of two inlets – for two different colored fluids – and two channels of different widths per inlet – one 250 μm and one 500 μm – and one relief channel per inlet. The fluidic channels were designed to accommodate one six-millimeter pin at each channel. All of the

channels meet at a viewing window where the fluid flow interactions can be viewed. After the viewing window is a gradient mixer to show more fluidic interactions. The user will be able to see the changes in fluid flow throughout the device depending on the configuration of the pins at each channel.

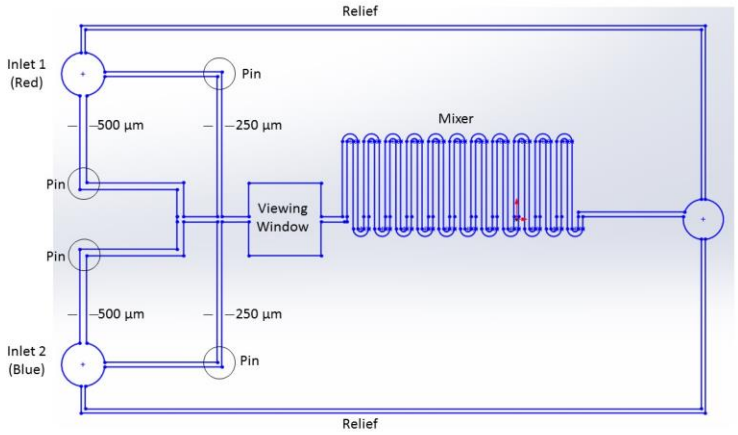

Figure 5.8.1. SolidWorks design of micro pin valve CFP.

The manufacturing of the pins was initially done by filling a well-plate with PDMS, as seen in Fig. 5.8.2. There were, however, issues with getting fully-formed pins out of the plate. The next iterations of pin valves were constructed from taking fully-cured PDMS and using a biopsy punch to create the desired pin size, as seen in Fig. 5.8.3. Finally, Fig. 5.8.4 shows the final pin configuration, which is the biopsy punch valves wrapped with tape to help prevent leaking.

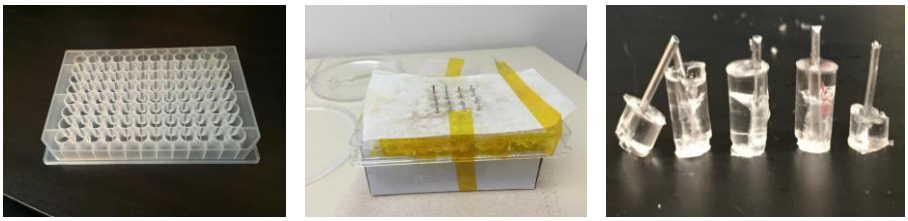

Figure 5.8.2. Well plate pin valve method and produced pins.

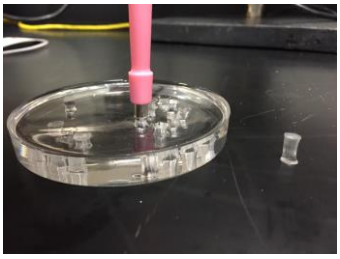

Figure 5.8.3. Biopsy punch pin valves.

Figure 5.8.4. Biopsy punch valves wrapped in tape.

5.8.3 Theoretical Analysis and Calculations

Due to the nature of what this device is testing, it is difficult to quantify the actual Reynolds number values; however, based on the Reynolds number analysis, Fig. 5.8.5, it is known that the smaller the channel width, the more turbulent the flow is. The analysis used the same equation and parameters as in section 5.5.4, but with a fluid flow of 30 µL/hr.

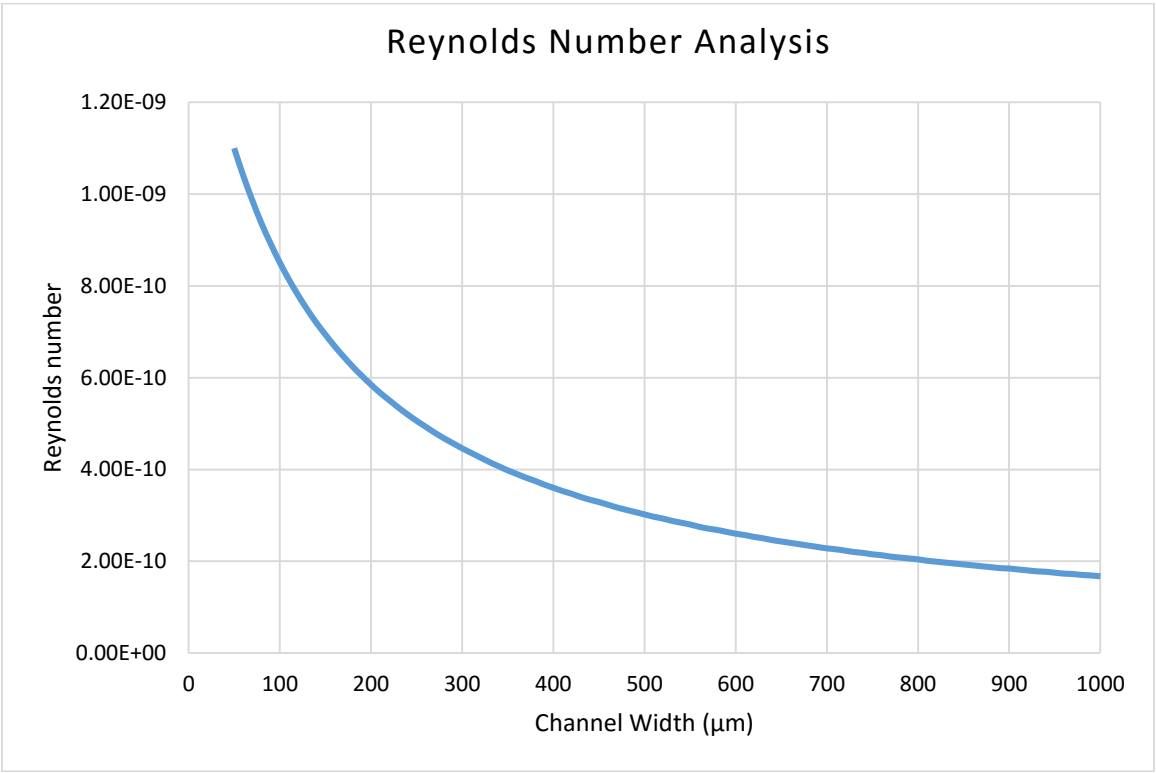

Figure 5.8.5. Reynolds Number analysis at 30 µL/hr.

After performing this analysis, two channel widths were chosen that show large differences in flow. Theoretically, when one fluid is flowing through the smaller channel and the other fluid is flowing through the larger channel, the former will be more turbulent, thus dominating the flow.

5.8.4 Testing Procedure

Two different colors, red and blue, were setup to flow at 30 µL/hr at each inlet. Then, the pins were oriented such that the red fluid was flowing through the 250 µm channel and the blue fluid was flowing through the 500 µm channel. Using the Keyence VHX-5000 Digital Microscope, photos were taken at the

viewing window to show how the fluids were interacting. Next, the pins were reversed: the red fluid flows through the 500 µm channel and the blue flows through the 250 µm channel. An RGB analysis was performed to see color values at different points across the viewing window. A datum was set at the bottom of the viewing window and RBG values were taken at 10 points along the viewing window until it reached the top. These values were compared to when red and blue are flowing through the same sized channels as a control.

5.8.5 Experimental Test Results

Fig. 5.8.6 shows the test results for the two different pin orientations, with another photo of fluids flowing through the same channel size as a control.

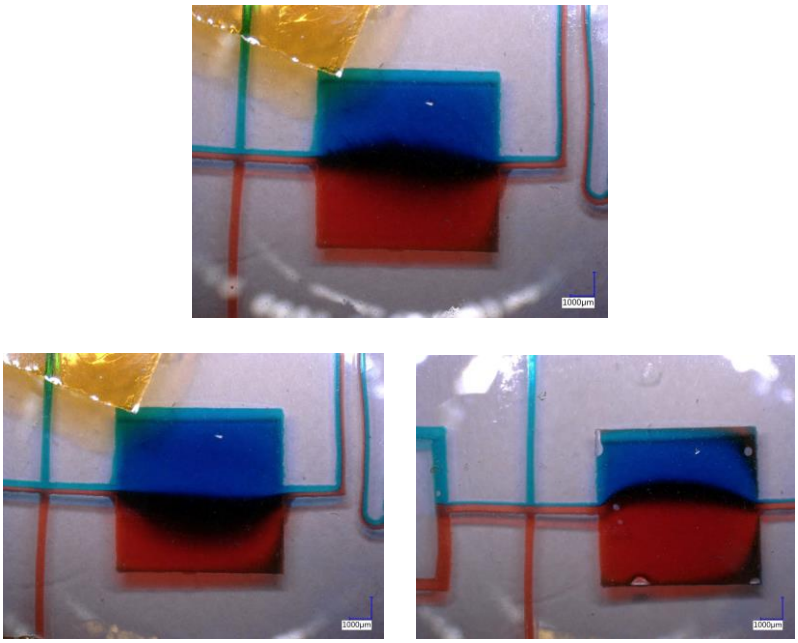

Figure 5.8.6. Top: Both red and blue fluids flowing through same size channel. Bottom: (Left) Blue flowing through 250 µm channel, red through 500 µm channel. (Right) Red flowing through 250 µm channel, blue through 500 µm channel.

As seen in the figures, the theoretical analysis holds true: the fluid that is flowing through the smaller channel dominates the flow of the fluid from the larger channel. Referring to the bottom left photo of Fig. 5.8.5, the blue is flowing through the smaller channel, making it relatively more turbulent than the red fluid flow. The apparent “curve” seen in the photo shows that there is more blue present in the lower half of the viewing window than red, and the same is true when the red fluid is flowing through the smaller channel. Table 5.8.1 shows an RGB analysis of red and blue values (ranging from 0 – 255, with 0 being no color and 255 being completely one color) across the viewing window and are compared to when the fluids are flowing through the same size channels

Table 5.8.1. RGB measurements across the viewing window. The 0 mm point is at the bottom of the viewing window and 5 mm is at the top.

Point on Viewing Window (mm)	Blue Dominate: (Blue/Red)	Red Dominate: (Blue/Red)	Equal Flow: (Blue/Red)
5 (Top)	171/0	150/3	182/6
4.5	145/2	131/5	156/6
4	138/2	125/4	141/1
3.5	137/3	41/0	139/2
3	133/3	0/0	74/3
2.5 (Middle)	92/4	9/89	0/0
2	0/0	9/115	4/61
1.5	2/16	9/111	6/95
1	2/70	10/115	8/108
0.5	10/104	10/110	14/123
0 (Bottom)	7/105	12/81	9/115

The results in Table 5.8.1 show that the fluid flowing through the smaller channel has a larger presence across the viewing window. For example, looking at the blue dominated column, there is a large presence of blue from the 5 mm point down to 2.5 mm, then the liquids diffuse at the 2 mm, meaning there is neither red nor blue present (0/0), and then the red color dominates down to 0 mm. The trend is the same for the red column: there is a large presence of red starting from the 0 mm point up to 2.5 mm, and then the liquids diffuse at 3 mm, and then blue dominates up to 5 mm. Comparing this to the equal flow column, the diffusion begins at 2.5 mm with an equal distribution of red and blue dominance above and below that point, thus showing that channel size affects the relative turbulence of the fluids.

Referring to Table 4.1 in the design specification section, the micro pin valves meet all of the applicable specifications. It meets the main specifications of being a safe, demonstrable, low cost, and easy-to-fabricate device that demonstrates scaling phenomena by user interactions, and is accompanied by an approved teaching module explaining hydrophobicity, equations used to model surface roughness, and real-world applications of this phenomenon. This device can be setup quickly, the pins and the device are both durable and can withstand multiple tests, and are small enough to have minimal packaging. This device also meets all of its device-specific specifications.

5.8.6 Final Design and Future Revision

The final design that was considered was similar to the CFP but with an additional inlet and more channels and pins. Appendix 9.4, Fig. 9.4.1 shows a SolidWorks drawing of the final design, and final product, Fig. 5.8.7, consists of three inlets, four channels of varying widths per inlet, and 12 total pin valves.

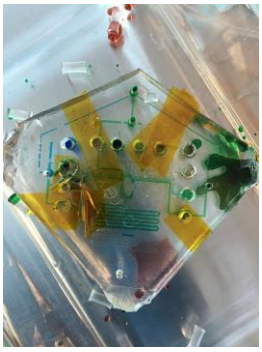

Figure 5.8.7. Physical device of proposed final design.

There were issues with this design: with too many moving components and pin valves, there were problems with pressure buildup, fluid flow, and leaking. The pin valves were unable to properly block the channels and allow fluid flow through the desired channels. Since the original CFP device was successful, with the addition of pin valves wrapped in tape and removal of relief channels (they were deemed unnecessary), that will be the final design of this device (Fig. 5.8.8). For future revisions, a different pin valve design would be considered, such as using a thin membrane to close channels, and have fewer channels per outlet.

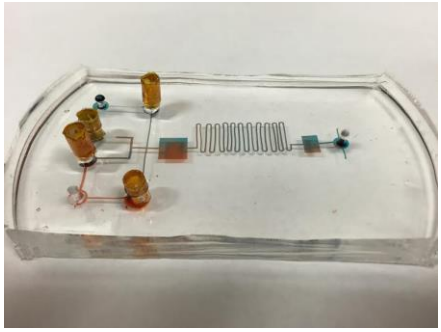

Figure 5.8.8. Final micro pin valve device.

5.9 Capillary Action

5.9.1 CFP Motivation

The purpose of this CFP was to demonstrate the maximum height to which fluid will flow through vertical micro-channels by capillary action as a function of channel widths. The measured heights are compared to the ones predicted by the derived theoretical models. Like all the other LOCs, the main goal of this device is to have an inherently high educational value by demonstrating a scaling phenomenon while being aesthetically pleasing and memorable.

5.9.2 CFP Conceptual Design

The CFP consists of multiple long, straight channels up to 80 mm in height with widths varying from 100 – 1500 µm, increasing by 100 µm per channel. The left edge of the device has a millimeter height gauge that will be used to determine the capillary height in each channel.

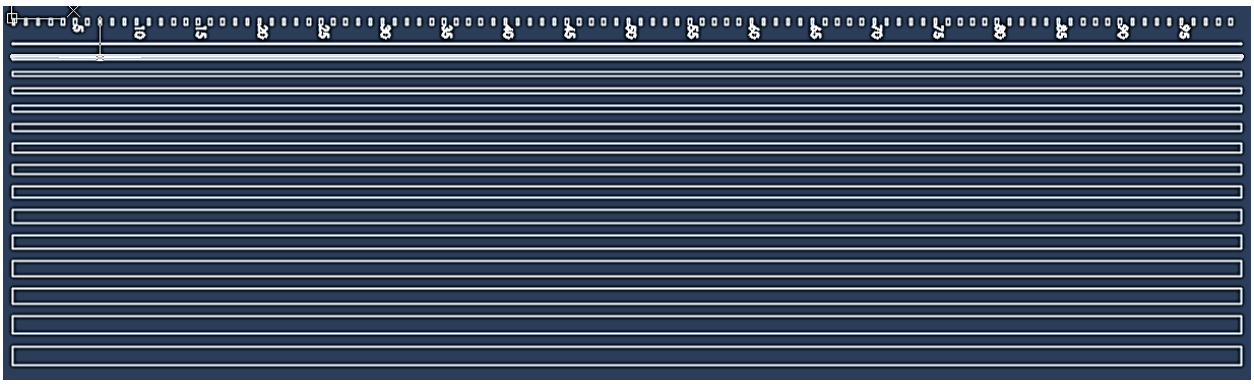

Figure 5.9.1. CAD drawing of capillary action CFP to test maximum fluid height. In order to show more detail, the device is shown rotate 90° clockwise. A millimeter bar will give a quick and rough visual measurement of the height.

5.9.3 Theoretical Analysis and Calculations

Intuitively, the height to which the fluid rises is expected to increase as the channel widths are decreased. The maximum height is reached when the forces from surface tension and adhesion are balanced by the weight of the fluid. A smaller channel results in a smaller fluid mass that leads to a greater height. The equation for determining the maximum height are typically only for circular tube. Since the channels in this device are rectangular due to the nature of the fabrication process, a new equation had to be derived from first principles.

The maximum fluid height h by capillary action in a rectangular channel is derived to be

$$h = \frac{2\gamma(t+w)}{\rho g t w} = \frac{2\gamma}{\rho g}\left(\frac{1}{t}+\frac{1}{w}\right) \tag{8}$$

where γ, t, w, ρ, and g represent the liquid-air surface tension of isopropyl alcohol, channel thickness, channel width, fluid density, and gravitational acceleration, respectively. Table 5.9.1 below describes all variables and their expected values. The only independent variable in the equation is the channel width since all other terms are to be constant.

Table 5.9.1. The parameters that determine the maximum fluid height and their values.

Description	Variable	Value
Fluid height	h	Dependent, expected 47 – 98 mm
Channel width	w	100 – 1500 µm
Channel thickness	t	130 µm
Surface tension of isopropyl	γ	0.0217 N/m
Density of isopropyl	ρ	786 kg/m^3
Gravitational acceleration	g	9.81 m/s^2

A very interesting result arises from the newly derived equation. It suggests there is a minimum height to which a fluid must rise regardless of how wide the channels become. Described in Eq. 9, as the value for channel width increases, the minimum limit of the height approaches a horizontal asymptote that is defined by the channel thickness. This minimum height is theoretically about 47 mm.

$$\lim_{w\to\infty} h = \frac{2\gamma}{\rho g t} \tag{9}$$

Conversely, the fluid height in a circular tube is simply related inversely to its width (diameter), so the height approaches zero with increasing width as shown below in the plot.

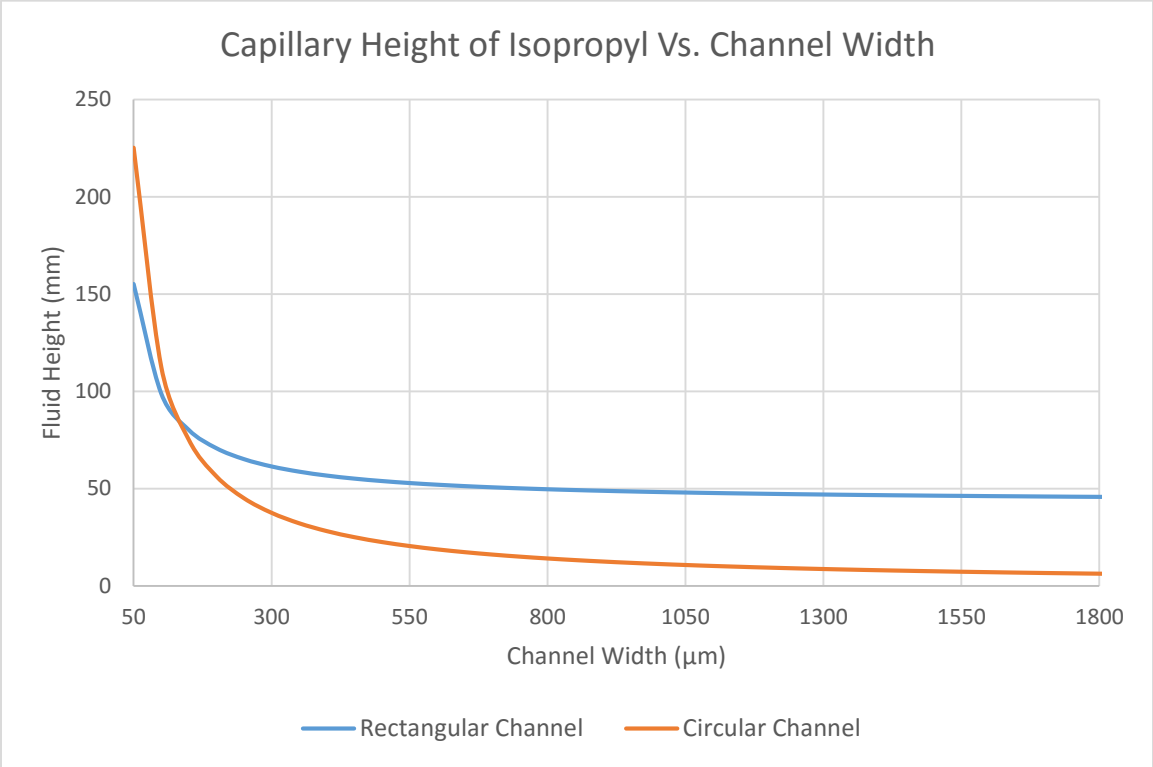

Figure 5.9.2. Capillary height of isopropyl vs channel width for rectangular and circular channels. The rectangular channels is expected to have a minimum height with increasing width whereas circular channels approach zero.

5.9.4 Testing Procedure

Since this device is relatively large compared to the other LOCs, it cannot be observed with the same microscope as the other devices. Instead, a DSLR camera with a macro lens will be used to image and record the capillary action device. One end of the device will be held vertically and dipped into a dish of isopropyl alcohol. An image will be taken at the end of capillary action and the height of each channel can be measured by the height bar as shown in Fig. 5.9.3.

5.9.5 Experimental Test Results

Excluding the first two channels, the other channels were able to exhibit the capillary action with an error of 6-8% from the theoretically anticipated behavior, shown in Fig. 5.9.4. The height of the meniscus within each channel is compared to the theoretical curve in Fig. 5.9.2. The major discrepancies from the first two channels could possibly be from channel leaking and blockages due to particle contamination, since they are only 100 – 200 µm wide. The main source of error from the other channels are likely due to idealized assumptions in the theoretical equation or slight variation in the values of variables such as fluid density and surface tension.

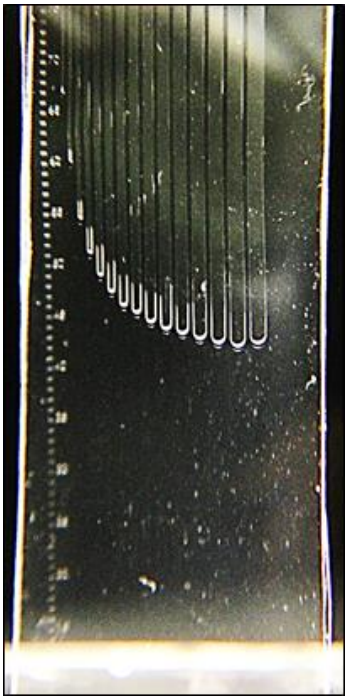

Figure 5.9.3. Capillary action device placed in a dish of isopropyl alcohol exhibiting the anticipated behavior in all 15 microchannels, including the asymptotic minimum height. The meniscus in each channel is measured relative to the height gauge on the left side.

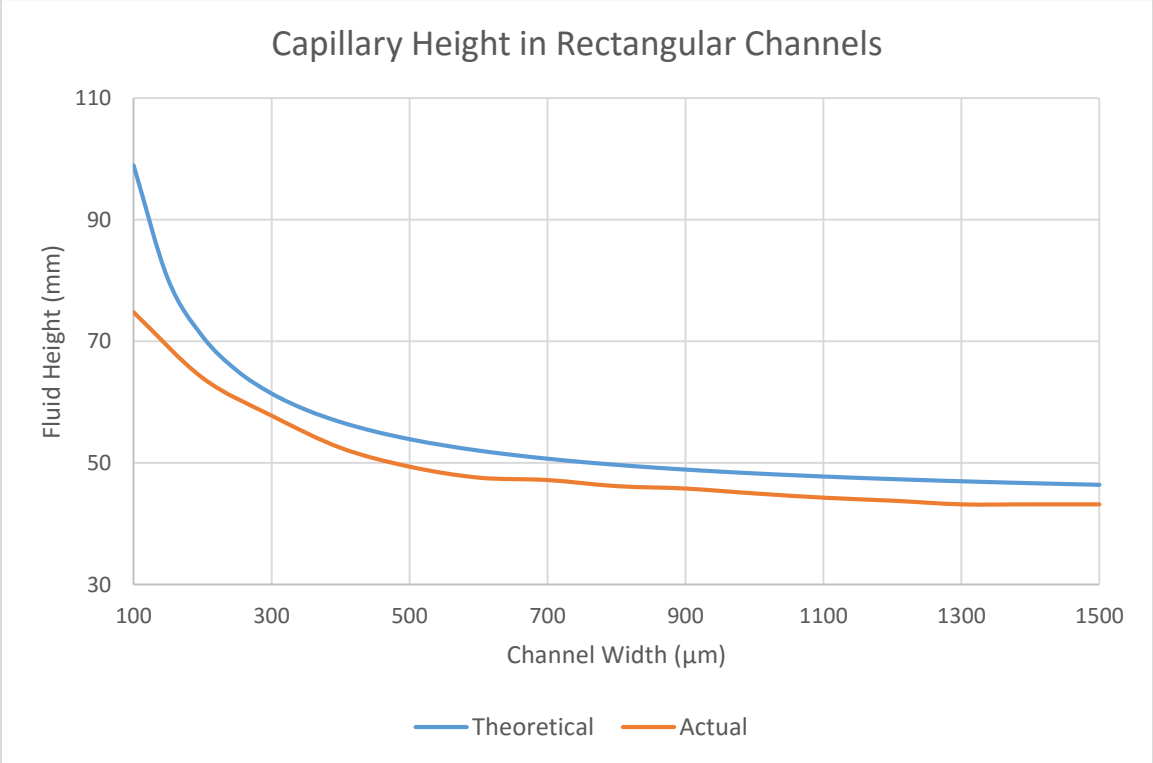

Figure 5.9.4. Plot of the actual capillary heights of the meniscus in each channel from Fig. 5.9.3 compared to the theoretical heights determined by Eq. 8. There is an error of about 6-8% from the theoretical curve, excluding the first two channels.

5.9.6 Final Design and Future Revision

This device was able to meet the goal of demonstrating the capillary action phenomena in rectangular microchannels as a function of channel widths and demonstrate the ability of the fluid in reach the theorized minimum height for the specified dimensions. The errors are considered small enough to be permissible and demonstrates the effects that idealized assumptions and approximations can have on actual results. No further work is planned for this device since it is considered functioning; however, knowledge of the device may be implemented different devices exhibiting the same phenomena.

5.10 Electrowetting

5.10.1 CFP Motivation

Electrowetting, more formally known as electrowetting-on-dielectric, is a phenomenon by which a hydrophobic surface can be made more hydrophilic by an applied electric field. This principle can also be used to manipulate to position of a water droplet. Most devices that exhibit electrowetting are designed to be closed systems where the water droplet is sandwiched between a dielectric and a ground plane that is optically clear but electrically conductive, as seen in Fig. 5.10.1. This design allows the device to be more durable since its thin-films are protected from direct contact. However, this type of system requires more development and manufacturing. A single-plane open system was selected since it is easier, quicker, and cheaper to fabricate but at the risk of damage and durability.

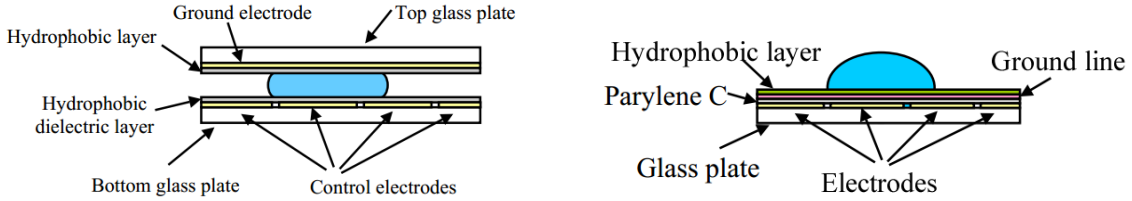

Figure 5.10.1. (Left) Example of an electrowetting closed system in which a droplet is sandwiched between two planes. (Right) Example of a typical open system using only a single plane. Parylene will serve as both the dielectric and hydrophobic layers.

5.10.2 CFP Conceptual Design

As described in the section 5.2.3 Electrowetting Fabrication steps, the device consists of three layers built on top a glass slide substrate within a cleanroom environment.

There are two rows of ten chromium electrodes each individually having lines leading to the edge for power contact points. All electrodes are 4 mm^2 and electrically isolated from one another by a 40 µm gap. The edges of each electrode consists of a zigzag pattern that interdigitates with a neighboring electrode shown in the Fig 5.10.3.

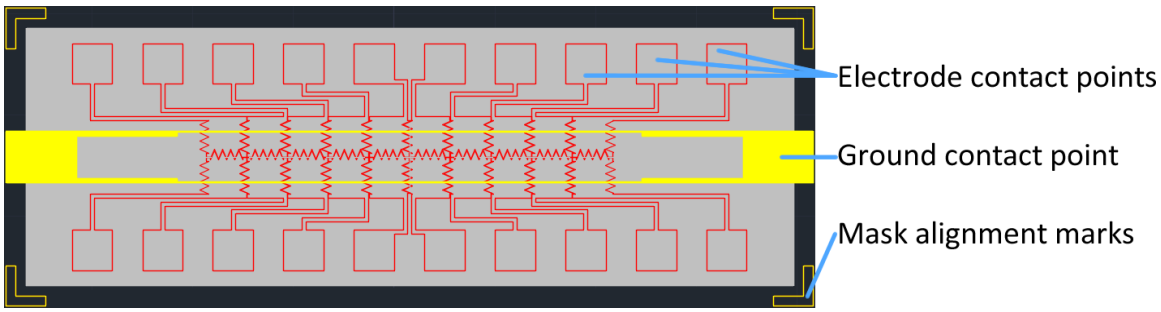

Figure 5.10.2. Top view CAD drawing of electrowetting device showing the two rows of electrodes and their contact points, the ground contact point, and the alignment marks for the photomasks.

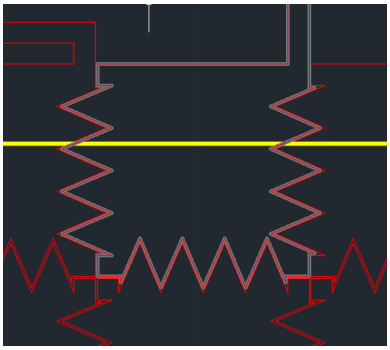

Figure 5.10.3. One electrode on device highlighted to show how it interdigitates with the surrounding electrodes. The thin bar spanning across the electrodes represents the grounding line. Another ground line off picture spans the lower row of electrodes.

The dielectric layer on electrowetting devices are typically coated with a thin film of Teflon to increase surface hydrophobicity. However, Teflon was extremely expensive and could not be justified in the budget. Instead, the Parylene doubled as a dielectric and slightly less hydrophobic layer.

One of the most critical parameters in this device is the thickness of the Parylene dielectric layer. A thicker dielectric will require a higher voltage. The CFPs will test the functionality of six different parameters: three thickness of Parylene (300, 600, and 900 nm) with two fabrication methods for the ground lines (positive resist and lift-off).

5.10.3 Theoretical Analysis and Calculations

The water droplet will have a contact angle >90° as it sits over a neutral electrode on a hydrophobic surface. A hydrophobic surface is necessary to allow the droplet to easily glide over the electrodes with minimal resistance.

When the electrode under the droplet is given a positive charge, there is a separation of charge in the Parylene layer such that the bottom of the layer is negative and the top is positively charged depicted in the figure below. The droplet, which is in contact with the grounding line, attains an overall negative charge and is flattened since it is attracted to the top of the positively charged Parylene. The resultant affect is that the hydrophobic layer is now more hydrophilic as the droplet contact angle decreases. If using an alternating current source, as with this device, the charge states in the layers and droplet will alternate at the same frequency outputted by the power source. By having interdigitated electrodes, a droplet will always be in contact with at least two other electrodes, allowing it to move towards an activated neighboring electrode.

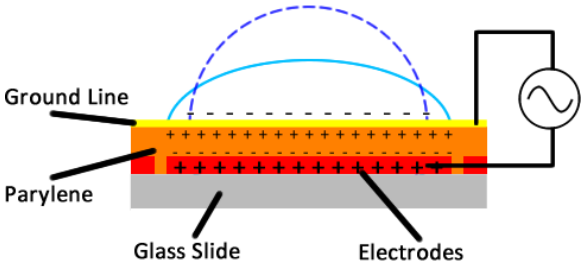

Figure 5.10.4. Cross-section diagram of the electrowetting device depicting the charge states within the layers. The charge flips at the same frequency as the power source.

The electrostatic force flattening the droplet down or pulling it laterally can be determined by the following equations.

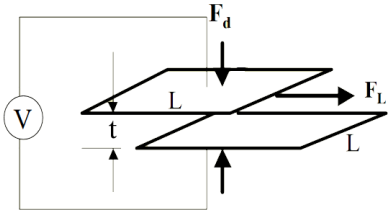

$$F_d = \frac{\varepsilon_0 \epsilon_r L^2 V^2}{2t^2} \quad (10)$$

$$F_L = \frac{\varepsilon_0 \epsilon_r L V^2}{2t} \quad (11)$$

Table 5.10.1. Parameters that determine the electrostatic force, their descriptions, and expected values.

Description	Variable	Value
Down, in-plane force	F_d	Dependent
Lateral force	F_L	Dependent
Permittivity of free space	ε_0	8.854×10^{-12} F/m
Relative dielectric permittivity	ε_r	3.15
Electrode side length	L	3 – 4 mm
Thickness of dielectric	t	300 – 1200 nm
Applied voltage	V	Independent, 55 – 110 V

The 50 µm wide and 50 nm thick ground lines does create an area over the Parylene where the topography is higher. However, since the width and thickness of the ground lines are so small relative to the area of the electrodes, they will not significantly affect the ability of the device to move droplets. It is possible to use electrowetting without a grounding line. In which case two consecutive electrodes are activated and the droplet is spread between them. This can leave the droplet with a residual charge even after the electric field is removed, potentially causing the droplet to resist moving to another pair of electrodes.

5.10.4 Testing Procedure

Since this is an open device, it is exposed to the particles in the air that need to be rinsed off with IPA, DI water, and dried with nitrogen gas before testing. The power source comes from a variable transformer capable of outputting up to 140 V. Since electrowetting uses only an electric field from an open circuit, no current is necessary so the power source is equipped with several Megohm resistors nearly eliminating any current. This will also prevent electrolysis of the droplet if pinholes are formed in the dielectric from physical damage or dielectric breakdown. On top of an electrode, a droplet of DI water of roughly the same size is place. The same electrode is activated to find the minimum voltage to see an

apparent change in droplet contact angle. A neighboring electrode is then activated to find the minimum voltage to achieve droplet displacement.

5.10.5 Experimental Test Results

All devices with ground lines fabricated using positive photoresist failed to displace a droplet at any voltage even up to the dielectric breakdown of all three thicknesses of Parylene. The Parylene loss all hydrophobicity and appeared to be very rough. This was likely caused during the physical vapor deposition phase when the hot chromium vapor precipitated on the Parylene surface, damaging it in the process.

The hydrophobicity of devices with ground lines formed by the lift-off method was retained since the Parylene surface was protected during the deposition process by photoresist. All these devices managed to show an apparent change in droplet contact angle. The devices with the two thicker dielectrics – 600 and 900 nm – were able to displace droplets.

Table 5.10.2. Results of different devices' ability to displace a droplet at some voltage. All devices with ground lines formed using positive resist failed, whereas devices formed using lift-off worked. The durability

Parylene Thickness (nm)	Positive Photoresist	Lift-off Photoresist
300	X	X
600	X	✓
900	X	✓

Table 5.10.3. Results of electrowetting device testing showing the voltages required for visible change in contact angle and droplet displacement as well as dielectric breakdown (22 V / 100 nm) for each thickness of Parylene.

Parylene Thickness (nm)	Voltages (V)		
	Contact Angle Change	***Displacement***	***Dielectric Breakdown***
300	55	X	66
600	60	75	132
900	70	85	198

After several sessions of testing, the 300 nm Parylene device stop functioning successful and the 600 nm soon followed. The 900 nm device lasted the longest but eventually stopped working as well. The initial thought was that hydrophobic properties of Parylene degrades over time depending on thickness. However, a published paper measured a nearly constant contact angle of droplets on Parylene over several weeks suggesting that Parylene does not lose its hydrophobicity over time (Brancato, et al.). Since the devices with the thickest layers of Parylene survived the longest, the cause for longevity is likely the durability of the Parylene to damage.

5.10.6 Final Design and Future Revision

The CFPs proved that the device design was viable but just needed more development. The final device consists of electrodes scaled down to 3 mm^2 and a Parylene layer that is 1200 nm. Several things about these two factors changes the performances of the device. First, a smaller droplet is required to cover the electrode area. The mass of the droplet is smaller and thus needs less force to move. Second, since the electrodes are smaller, they produce a smaller electrostatic force. Third, the thicker layer of Parylene improves to durability of the hydrophobic surface, but more voltage is necessary since the gap between the droplet and electrode is greater.

It can be shown that the mass of the water droplet scales down much faster than the electrostatic force by which the droplets are manipulated. Calculations using the Eq. 11 and the approximation that the droplets are hemispheres show that the ratio of force to mass for the final device is greater than that of the CFP.

$$F_{L,CFP} = \left(\frac{\varepsilon_0 \epsilon_r}{2}\right)\frac{L_1 {V_1}^2}{t_1} = \left(\frac{\varepsilon_0 \epsilon_r}{2}\right)\frac{(4x10^6\ nm)(85V)^2}{900\ nm}$$

$$F_{L,Final} = \left(\frac{\varepsilon_0 \epsilon_r}{2}\right)\frac{L_2 {V_2}^2}{t_2} = \left(\frac{\varepsilon_0 \epsilon_r}{2}\right)\frac{(3x10^6\ nm)(110V)^2}{1200\ nm}$$

$$\frac{F_{L,CFP}}{F_{L,Final}} = 1.06$$

The 110 V was experimentally determined after the fabrication of the final device. This happens to be the voltage that nearly provides the same force in the final device as with the CFP. The electrostatic force essentially stayed the same with the new electrode size and parylene thickness.

$$m \propto V = \frac{\pi L^3}{12}$$

$$V_{CFP} = \frac{\pi {L_1}^3}{12} = \frac{\pi(4\ mm)^3}{12}$$

$$V_{Final} = \frac{\pi {L_2}^3}{12} = \frac{\pi(3\ mm)^3}{12}$$

$$\frac{V_{CFP}}{V_{Final}} = 2.37$$

Mass is proportional to volume by density which is constant. The volumetric ratios of the droplets are relatively large due to the cubic rate of scaling. This larger rate of scaling allows the force to mass ratio in the final device to be much greater than that of the CFP resulting in a more functioning design.

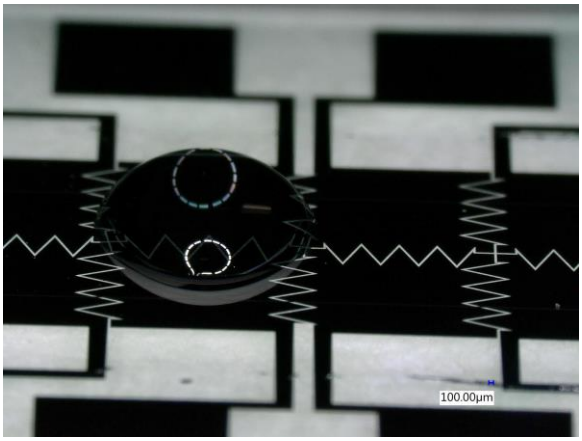

Figure 5.10.5. Image from an optical microscope of the final electrowetting device design.

The design is essentially finished and meets the global specifications for all devices and those particular to this device except for durability and inlet/outlet ports (Tables 4.1 and 4.9). Durability is something that cannot be solved simply due to the nature of having an open system device, which was selected over a protected closed system to meet the need to easy of manufacturing. Taking care never to physically contact the hydrophobic surface with anything other than water or cleaning fluids will prolong the functionality of the device. The number of inlet and outlet ports are not applicable to this device

If more funds are budgeted for this device in the future, further development of this device can be designed on a larger substrate with more intricate electrode layouts. The device could even incorporate a microcontroller to displace water droplets autonomously.

6.0 Project Planning

6.1 Schedule

In order to have eight LOC devices ready for design day, a thorough and detailed schedule of major milestones was created, which can be seen in the next two sections. Detailed descriptions of each task are included in the fall and spring sections, and a design structure matrix chart is found at the end of project planning.

6.1.1 Fall Semester

Table 6.1.1. List of dates for important milestones in the fall 2015 semester.

Date	Milestone
September 23	Review of CAD drawings of chip designs by advisor
September 30	Begin laser prototyping of chips
October 5	CFP Motivation Presentation
October 7	Review design and incorporate feedback from CFP Presentation
October 30	Fabrication of second-round design
November 6	Simulation of devices
November 13	First draft of scaling-law presentation
November 13	Finalize CFP demonstration
November 16	**CFP Presentation**
November 27	Final scaling-law presentation
December 7	Final iteration of first device
December 11	**Final Project Report**

6.1.2 Spring Semester

Table 6.1.2. List of dates for important milestones in the spring 2016 semester.

Date	Milestone
January 22	Complete designs for second device
January 25	Share first semester presentations
February 8	**Design review 1**
February 10	Initial prototypes tested
February 12	Second iteration of device prototypes designed
February 26	Second iteration prototypes tested
March 4	Finalize second device design
March 7	**Design Review 2**
March 18	Fabrication of second device
March 23	Testing of second device
April 6	**Design day poster – final draft**
April 6	**Design review 3**
April 11	Final fabrication of all devices
April 13	Finish second device presentation
April 18	Finalize packaging
April 21	**Design Day**
April 26	**Final report due**

6.1.3 Design Structure Matrix

Table 6.1.3. Updated Design Structure Matrix for fall and spring semester.

Task		A	B	C	D	E	F	G	H	I	J	K	L	M	N	O	P	Q	R	S	T	U	V
Understand the nature of our project	A	A																					
Determine customer needs	B	X	B																				
Nanofab training course	C	X		C																			
Create a budget	D		X		D																		
Document scaling phenomenon	E	X	X	X		E																	
Determine critical functions	F		X	X	X		F																
Model critical functions	G						X	G															
Start fab. of design prototypes	H				X	X	X		H														
CFP motivtional presentation	I	X	X		X	X	X	X	X	I													
Fabrication of CFP prototypes	J									X	J												
Test critical function	K										X	K											
Review device designs	L											X	L										
Improve on design	M												X	M									
CFP presentation	N							X			X	X	X		N								
Final iterations on first device	O												X	X		O							
Final project report	P														X		P						
Work iterations on second device	Q															X		Q					
Design packaging	R																		R				
Presenting devices	S																		X	S			
Go to schools for feedback on devices	T																	X	X		T		
Improve designs	U																				X	U	
Fabrication and final testing	V																					X	V

6.2 Budget

The majority of the budget spent in the fall 2015 semester pertains mostly to one time startup costs such as syringe pumps, tubing, fittings, fluids, and other supplies which are not expected to be purchased again. The money they was spent in excess to the anticipated costs was taken from the next semester's budget. However, the remaining budget for the spring 2016 semester was sufficient since most of the costs will go towards paying for time on the machines in the Nanofab.

Table 6.2.1. Available funds from class fees and the Nanofab KECK fund.

	Fall 2015	Spring 2016
Anticipated Budget	$3200	$1000 - $260
Actual Amount Spent	$3460	$702.77
Over Budget	($260)	-
Remaining	$0	$37.23

Table 6.2.2. Supplies and quantities necessary for fabricating the LOC's, along with allocation of class and KECK funds and total cost during Fall 2015 Semester.

Supplies/Tool	Price	Quantity	Total	Fund	Description
Desiccator	$ 101.70	1	$ 101.70	ME	Vacuum desiccator for PDMS
Petri Dishes	$ 19.98	1	$ 19.98	ME	Set of petri dishes for holding PDMS
Additional Fittings	$ 21.40	1	$ 21.40	ME	Additional barbed fitting connectors
Mixing Bowls	$ 21.99	1	$ 21.99	ME	Disposable mixing bowls for PDMS
TWEEN 20	$ 18.40	1	$ 18.40	ME	Emulsifying agent for water
SU8 Photoresist	$ 459.00	1	$ 459.00	Keck	Negative photoresist to make molds
Photomasks	$ 23.70	3	$ 71.10	Keck	Photolithographic masks for designs
Mask Maker Time	$ 41.00	12	$ 492.00	Keck	Cost of running mask maker per hour
PDMS 0.5 kg	$ 42.99	1	$ 42.99	Keck	DC 184 SYLGARD Encapsulant PDMS 0.5 kg
PDMS 3.9 kg	$ 356.18	1	$ 356.18	Keck	DC 184 SYLGARD Encapsulant PDMS 3.9 kg
Silicon Wafers	$ 15.65	10	$ 156.50	Keck	4 inch Silicon wafers
Biopsy Punches	$ 84.50	1	$ 84.50	Keck	Various diameters of biopsy punches
Cutting Mat	$ 5.00	1	$ 5.00	Keck	Cutting mats for biopsy punches
Syringes	$ 35.00	1	$ 35.00	Keck	Various luer syringes kit from 1-60 mL
Tubing	$ 41.75	1	$ 41.75	Keck	Different tubing materials
Fittings/Locks	$ 23.75	1	$ 23.75	Keck	Luer locks and barbed fittings
Syringe Pump	$ 259.99	2	$ 519.98	Keck	Infusion-only, non-programmable syringe pump
Syringe Pump	$ 928.00	1	$ 928.00	Keck	More accurate, programmable syringe pump
SU8 Spinner	$ 62.00	1	$ 62.00	Keck	SU8 spinner tool, cost/hr
Total			**$ 3,461.22**		

Table 6.2.3. Supplies and costs used during Spring 2016 Semester.

Supplies/Tool	Price	Quantity	Total	Fund	Description
Vinyl Tape	$ 61.66	1	$ 61.66	ME	Vinyl transfer tape for molds
Petri Dishes	$ 10.95	1	$ 10.95	ME	Petri Dishes 100 mm
Petri Dishes	$ 13.07	1	$ 13.07	ME	Petri Dishes 120 mm
PDMS 05 kg	$ 42.99	1	$ 42.99	Keck	PDMS Elastomer
Photomask	$ 23.70	3	$ 71.10	Keck	5 inch photomask
Mask Maker	$ 41.00	4	$ 164.00	Keck	Mask maker hourly rate
Evaporator	$ 46.00	4	$ 184.00	Keck	Evaporator hourly rate
Parylene	$ 31.00	5	$ 155.00	Keck	Parylene coater hourly rate
Total			**$ 3,461.22**		

7. Conclusions

7.1 Summary

Eight microfluidic LOC devices were successfully designed and fabricated, all demonstrating scaling laws and real-world applications. All of the devices meet the required design and customer specifications, unless noted otherwise. For the devices that do not meet certain expectations, explanations of future revisions have been noted in their respective sections. Each device is accompanied with advisor-approved teaching modules that explain the physics, design, and applications of the LOCs. Overall, an array of teachable, demonstrable, and low-cost devices was successfully procured for high school and college-level science courses.

7.2 Future Work

For future work, the LOCs need to be consolidated and properly kitted to send out to customers. Right now, all of the devices can be individually packaged and all of the teaching modules have been consolidated. Future work for specific devices has been discussed in the individual device sections. The next step for this project would be to get more funding to execute the proper changes that are necessary for each device and to create an organized, compact kit of all of the LOC devices to be distributed to interested customers.

8. Reference Materials

8.1 Referenced Articles

Gartner, Claudia, “microfluidic ChipShop Lab-on-a-Chip Catalogue”, catalogue, 2011

Hake, R. (1998). Interactive-engagement vs traditional methods: A six-thousand-student survey of mechanics test data for introductory physics courses *American Journal of Physics,* 66, 64-74.

Hemling, Melissa, John A. Crooks, Piercen M. Oliver, Katie Brenner, Jennifer Gilbertson, George C. Lisensky, and Douglas B. Weibel. "Microfluidics for High School Chemistry Students." *J. Chem. Educ. Journal of Chemical Education* (2014): 112-15. Print.

Microflexis. Web. 23 Nov. 2015. <www.microflexis.com>

"Nanotechnology Careers." *National Nanotechnology Infrastructure Network*. Web. 10 Dec. 2015.

thinXXS Microtechnology. Web. 23 Nov. 2015. <www.thinxxs.com>

Y. Zhang, L. Wang, “Microfluidics: Fabrication, Droplets, Bubbles, and Nanofluids Synthesis”, Advances in Transport Phenomena, ADVTRANS 2, pp.171-294, 2011

Brancato, L., et al., “Plasma enhanced hydrophobicity of parylene-C surfaces for a blood contacting pressure sensor”, EUROSENSORS 2014, pp. 4, 2014

9. Appendices

9.1 Appendix - Micro-droplet Formation

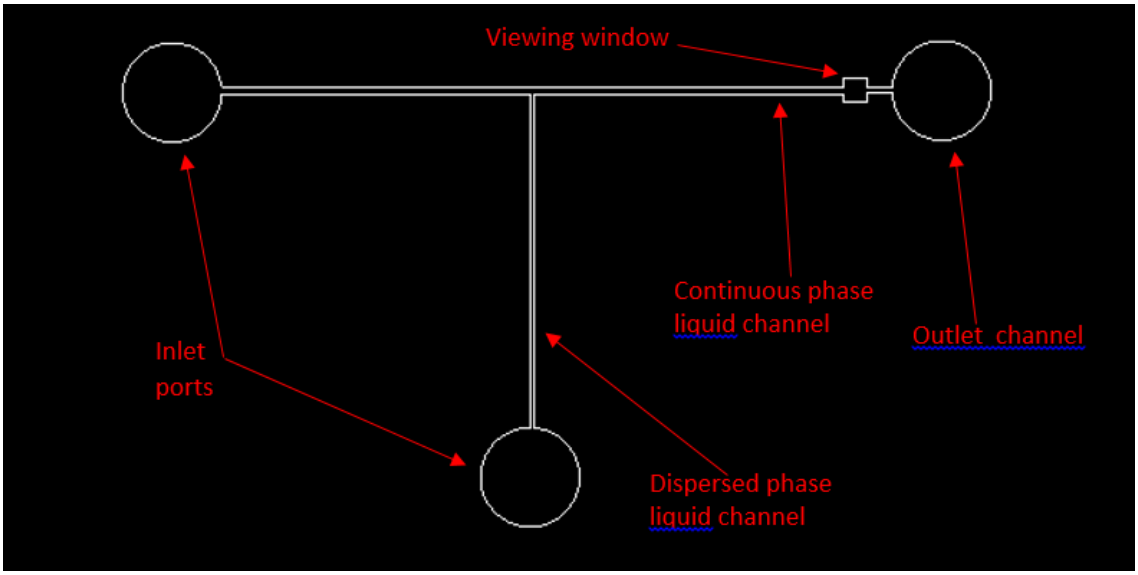

Figure 9.1.1. Geometry used for micro-droplet formation CFP.

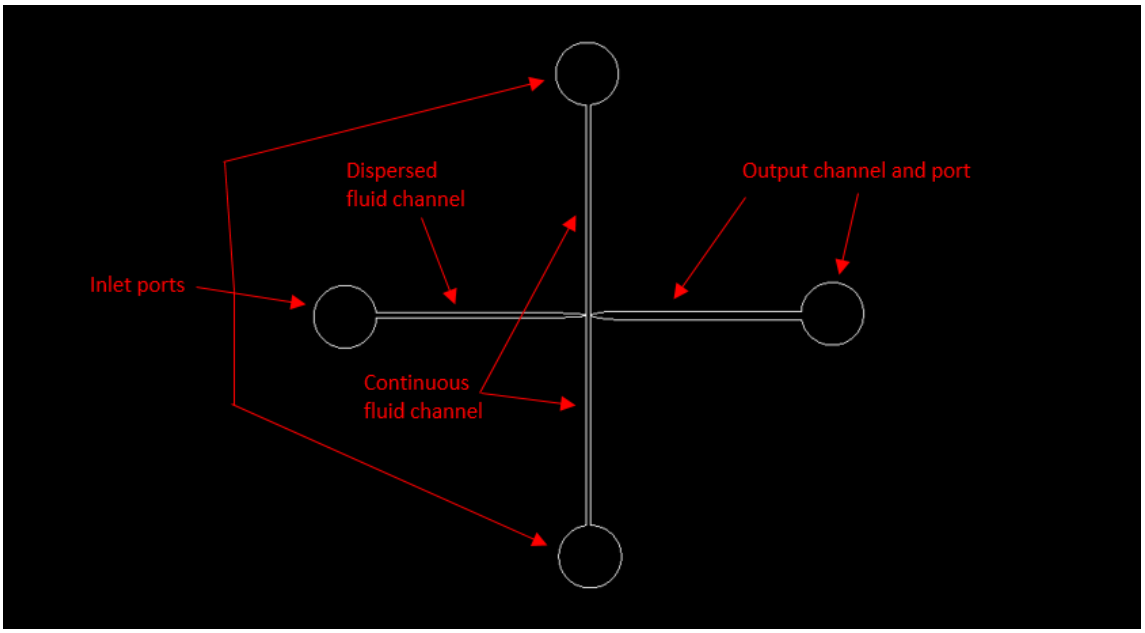

Figure 9.1.2. Final design geometry used for micro droplet formation.

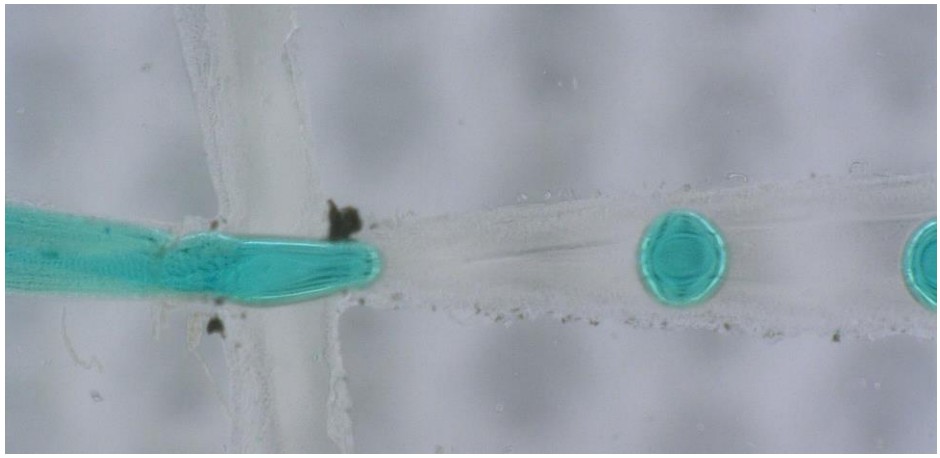

Figure 9.1.3. Micro droplet formation using final design geometry.

9.2 Appendix - Gradient Mixer

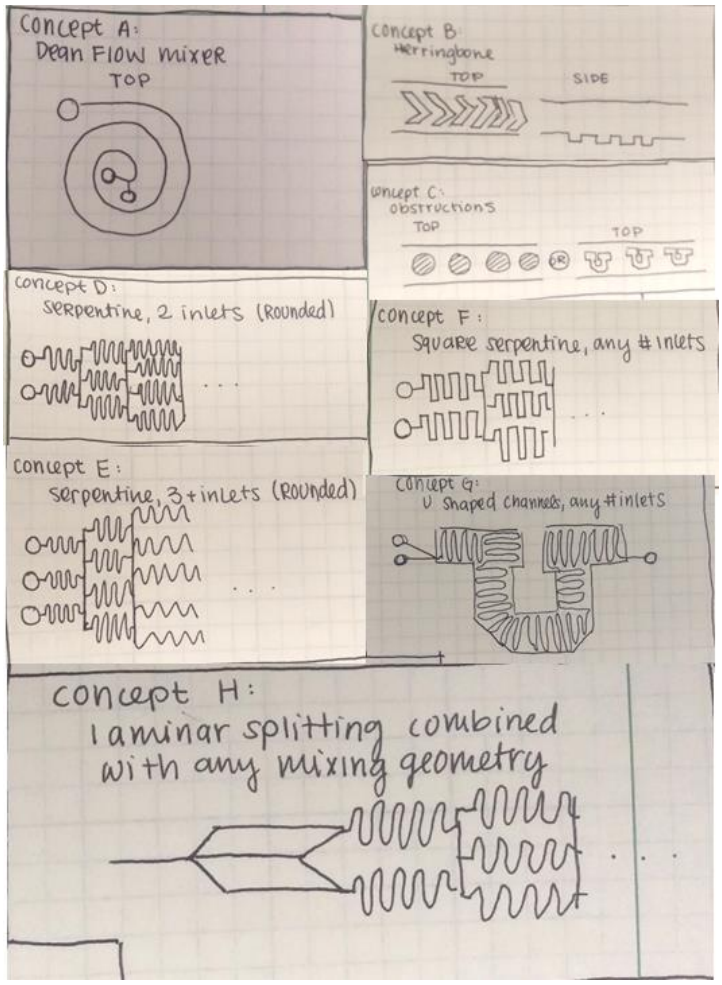

Figure 9.2.1. Design concepts for gradient mixer brainstorming design matrix.

Table 9.2.1. Design matrix for gradient mixer brainstorming. See Fig. 9.2.1 for Concept Variant clarification.

	Concept Variants								
Selection Criteria	**A**	**B**	**C**	**D**	**E**	**F**	**G**	**H**	**Ref**
Ease of fabrication	0	-	0	+	+	+	-	+	0
Unique geometries	+	+	+	0	0	0	+	+	0
Ability to mix	-	0	0	+	+	+	+	+	0
Pluses	1	1	1	2	2	2	2	3	
Sames	1	1	2	1	1	1	0	0	
Minuses	1	1	0	0	0	0	1	0	
Net	0	0	1	2	2	2	1	3	
Rank	4	4	3	2	2	2	3	1	
Continue?	No	No	Yes	Yes	No	Yes	No	Yes	

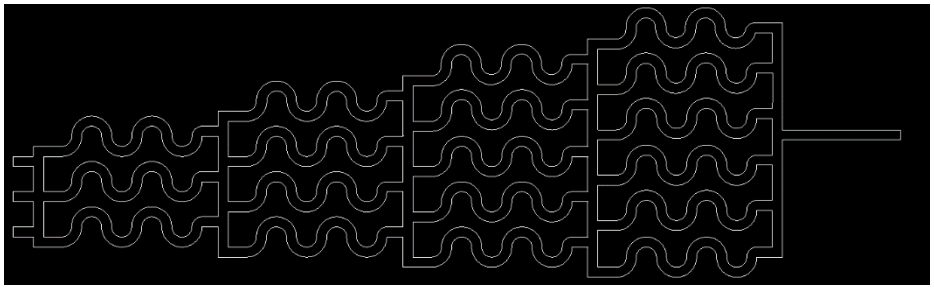

Figure 9.2.2. First prototype of gradient mixing channels

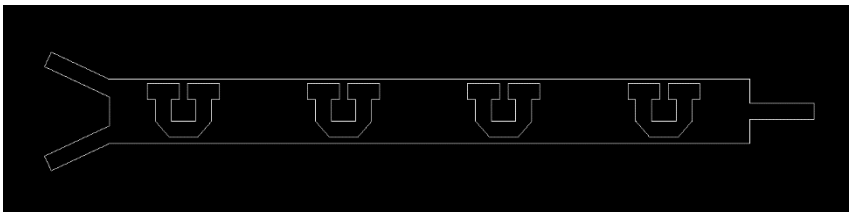

Figure 9.2.3 First prototype of blockade mixing channel

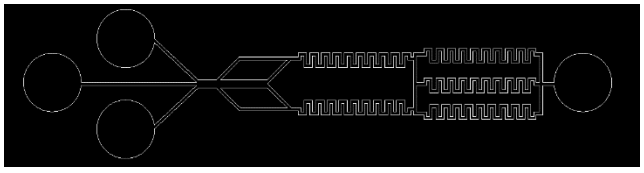

Figure 9.2.4 First prototype of laminar splitting channel

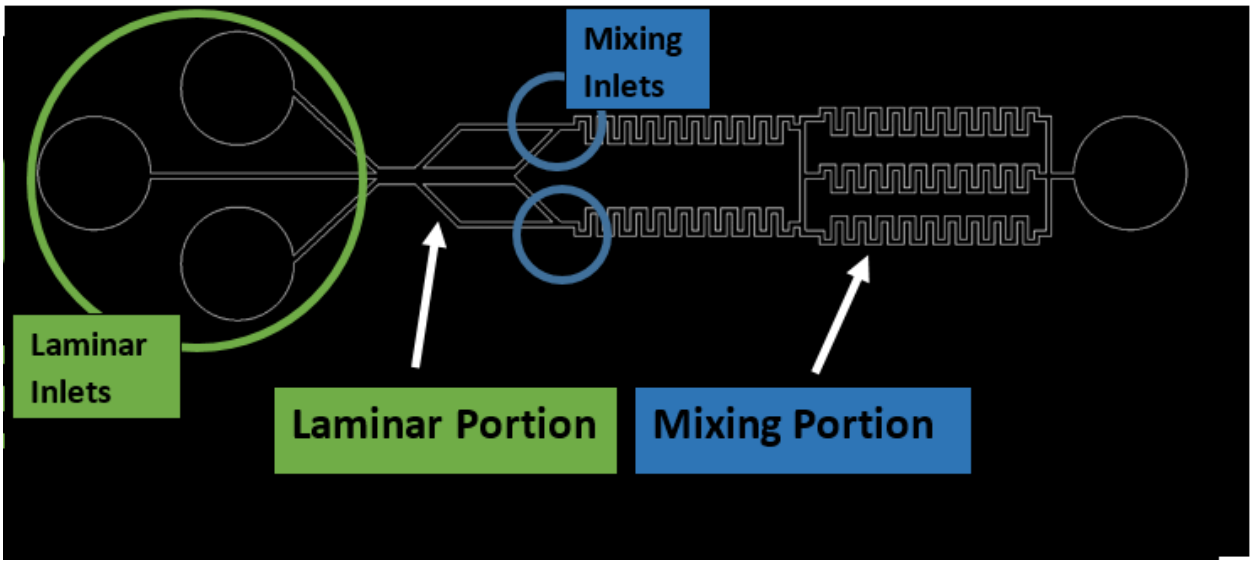

Figure 9.2.5. Prototype of gradient mixer LOC. On the left hand side, the laminar portion is supplied by three external inlets powered by syringe pumps. On the right hand side, the mixing portion of the device is supplied by two "inlets" of fluid coming from the laminar portion of the device.

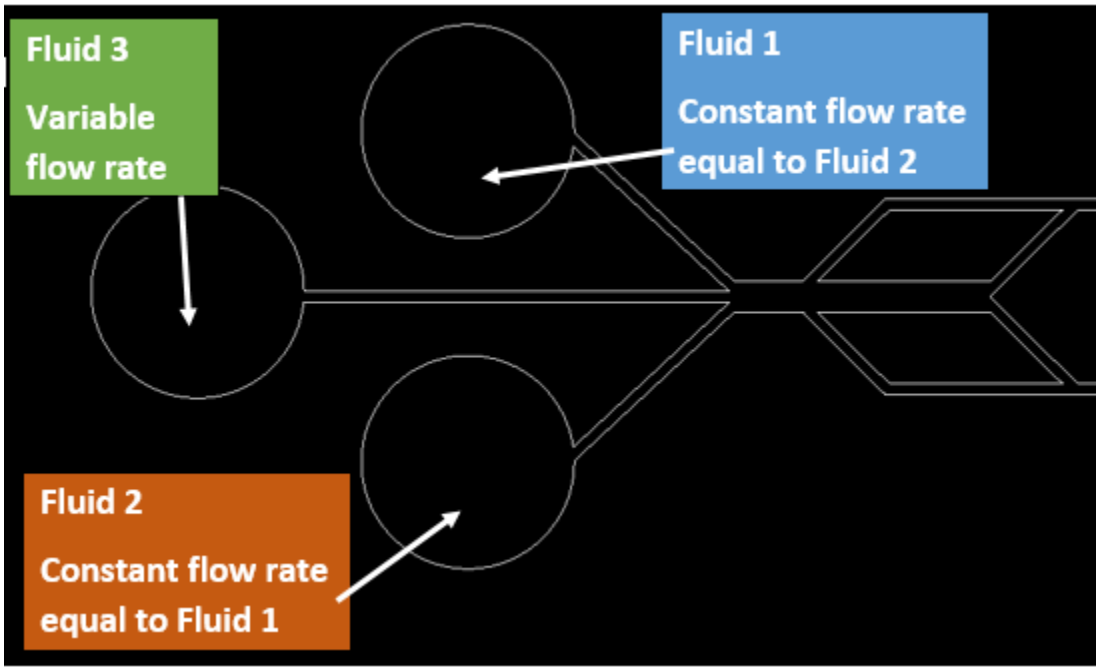

Figure 9.2.6. Laminar portion of gradient mixer prototype. The center inlet, where Fluid 3 enters the device, will be variable. Fluid 1 and Fluid 2 will enter the device at constant flow rates equal to one another. Each fluid will be a different color.

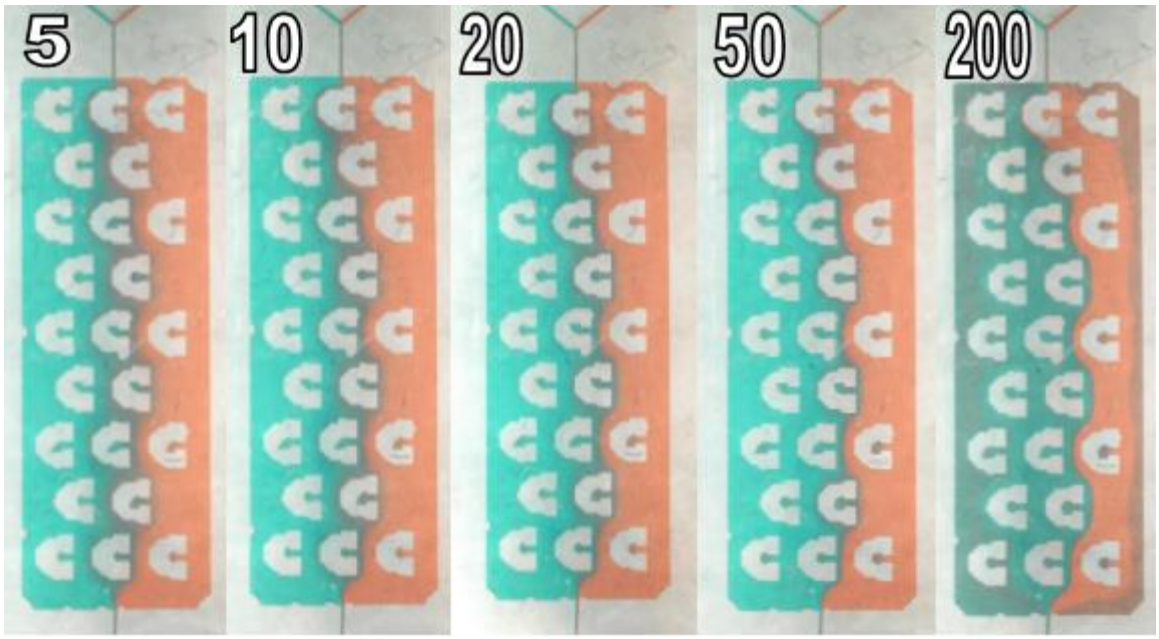

Figure 9.2.7. Mixing results from horizontal blockade channel. The numbers represent the flow rate in µL/min.

Figure 9.2.8. Mixing results from vertical blockade channel. The numbers represent the flow rate in µL/min.

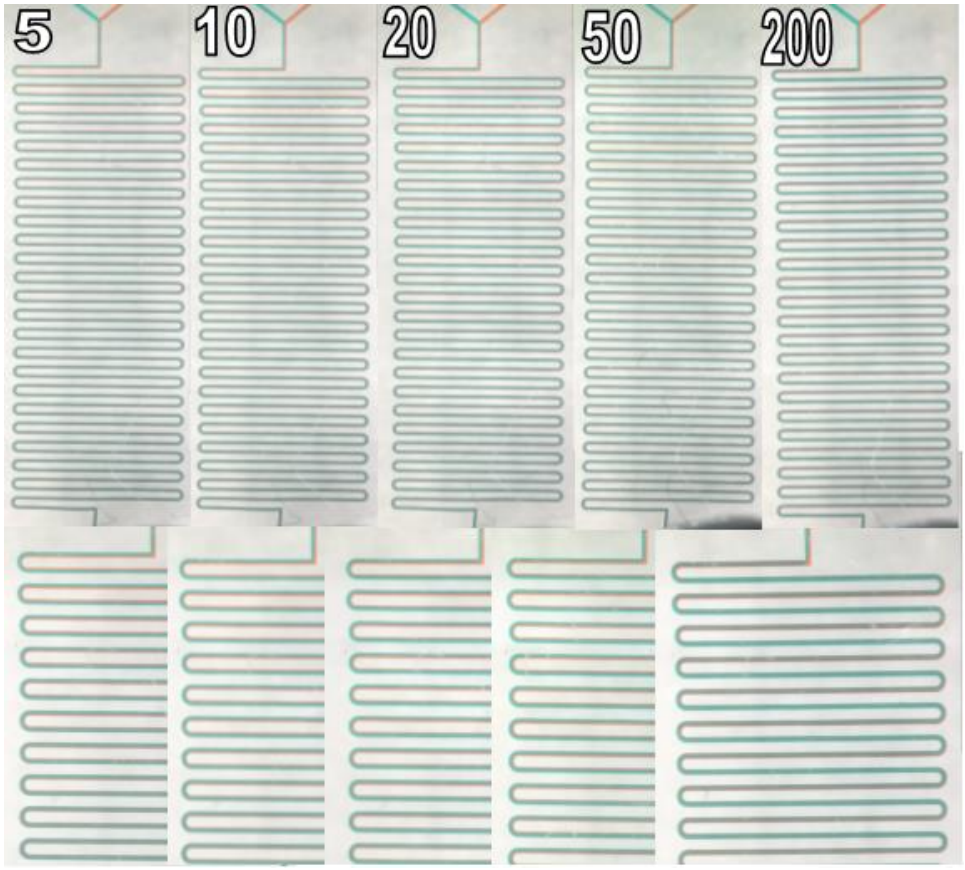

Figure 9.2.9. Mixing results from rounded serpentine channel with zoomed in view below. The numbers represent the flow rate in µL/min.

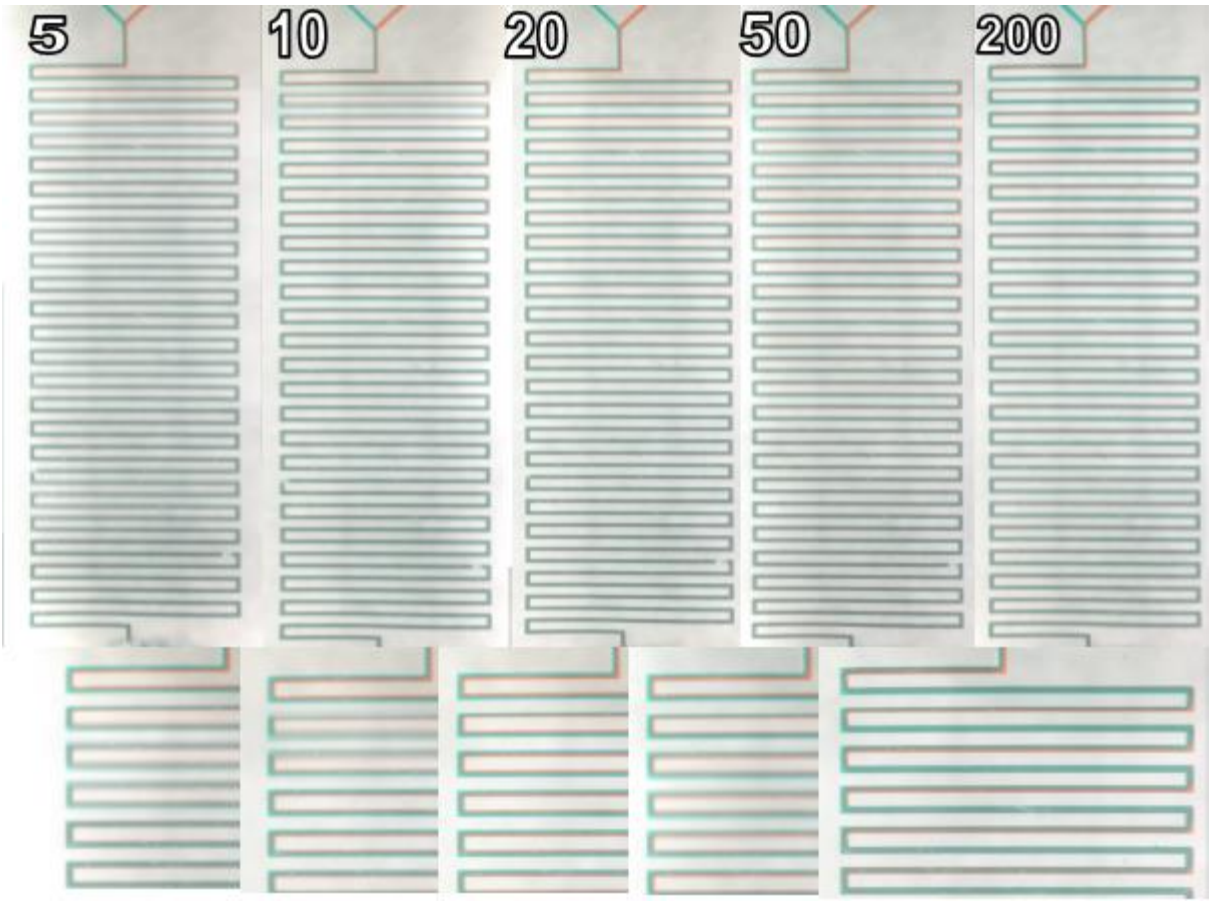

Figure 9.2.10. Mixing results from square serpentine channel with zoomed in view below. The numbers represent the flow rate in µL/min.

Table 9.2.2. Raw RGB values at outlet for flow rate of 5 µL/min.

Red Initial			**Blue Initial**			**Vertical Blockade**			**Horizontal Blockade**			**Round Serpentine**			**Square Serpentine**		
R	**G**	**B**	**R**	**G**	**B**	**R**	**G**	**B**	**R**	**G**	**B**	**R**	**G**	**B**	**R**	**G**	**B**
218	150	123	98	195	181	111	152	146	219	138	109	140	152	148	138	163	157
217	136	109	73	182	162	209	148	117	89	165	155	116	141	137	123	144	137
204	137	113	80	183	169	100	181	172	106	143	136	138	162	153	130	153	147
224	152	118	77	188	169	173	144	136	210	135	106	114	137	131	141	160	154
211	135	106	66	173	155	133	142	139	102	158	149	129	152	146	136	155	151
202	134	107	74	183	165	78	191	173	187	130	110	123	145	142	169	176	169
208	141	106	87	186	175	141	143	142	86	138	126	134	143	140	139	156	150
205	135	104	83	190	173	198	135	104	207	136	108	127	149	146	133	155	143
214	144	115	95	188	173	140	143	134	93	165	153	130	147	141	149	172	166
222	146	117	78	187	169	190	143	123	151	142	133	119	140	135	144	163	159

Table 9.2.3. Raw RGB values at outlet for flow rate of 10 µL/min.

Red Initial			Blue Initial			Vertical Blockade			Horizontal Blockade			Round Serpentine			Square Serpentine		
R	**G**	**B**	**R**	**G**	**B**	**R**	**G**	**B**	**R**	**G**	**B**	**R**	**G**	**B**	**R**	**G**	**B**
186	120	96	57	168	151	205	141	114	92	148	139	117	142	136	136	155	151
187	123	98	71	187	168	198	148	123	183	138	119	150	162	158	128	149	144
186	132	104	58	170	154	100	184	168	77	161	148	131	140	137	150	159	154
184	124	96	73	168	148	185	149	127	134	124	122	133	148	143	123	144	137
195	134	106	68	176	161	87	191	180	68	183	170	142	153	149	133	154	147
190	135	105	68	170	156	133	146	139	203	128	105	127	139	135	139	158	154
192	132	104	63	175	159	174	159	140	115	173	161	132	147	142	132	153	148
189	123	97	48	159	143	209	144	116	119	146	141	127	146	144	133	159	150
191	134	117	44	172	147	101	194	183	127	145	145	128	145	139	153	168	163
191	125	99	67	182	155	207	151	128	195	136	118	140	152	148	133	154	149

Table 9.2.4. Raw RGB values at outlet for flow rate of 20 µL/min.

Red Initial			Blue Initial			Vertical Blockade			Horizontal Blockade			Round Serpentine			Square Serpentine		
R	**G**	**B**	**R**	**G**	**B**	**R**	**G**	**B**	**R**	**G**	**B**	**R**	**G**	**B**	**R**	**G**	**B**
195	133	96	71	177	157	93	193	181	64	172	157	157	163	159	136	151	146
176	128	90	73	176	159	211	147	119	190	138	127	142	151	148	139	150	146
196	137	107	64	167	150	153	144	135	46	163	144	118	154	144	111	132	127
207	142	110	68	180	164	122	151	146	183	118	100	134	146	142	148	159	155
192	133	99	76	175	157	187	158	128	205	132	113	130	157	150	118	139	134
185	124	95	96	184	170	210	150	116	108	175	165	141	150	149	129	148	142
198	135	102	71	168	151	78	185	169	113	119	115	133	144	140	120	137	131
193	140	108	77	171	155	202	135	106	73	170	159	127	157	149	123	142	138
192	126	94	69	171	157	172	149	133	200	132	109	145	157	153	144	156	152
191	139	118	45	156	139	87	192	177	168	135	130	130	151	146	125	137	133

Table 9.2.5. Raw RGB values at outlet for flow rate of 50 µL/min.

Red Initial			Blue Initial			Vertical Blockade			Horizontal Blockade			Round Serpentine			Square Serpentine		
R	G	B	R	G	B	R	G	B	R	G	B	R	G	B	R	G	B
171	125	92	69	185	172	202	145	118	142	129	121	129	138	135	124	141	135
168	131	102	57	168	151	193	148	117	64	175	159	117	150	141	146	146	144
200	144	117	46	157	141	89	181	166	150	140	128	138	140	139	128	147	143
195	131	104	78	175	164	96	201	184	210	139	111	134	145	141	134	140	136
183	126	96	59	166	156	168	143	139	129	130	124	137	146	143	126	136	137
193	133	107	54	169	152	111	163	158	72	180	165	127	154	147	153	152	148
185	124	95	61	182	163	202	145	126	202	137	109	127	139	135	145	147	142
186	126	98	55	170	153	90	187	170	139	140	134	130	136	134	131	137	133
178	125	93	63	173	162	195	134	116	109	141	140	126	137	133	129	144	141
185	145	119	63	173	160	138	148	149	177	132	127	133	165	154	141	146	140

Table 9.2.6. Raw RGB values at outlet for flow rate of 200 µL/min.

Red Initial			Blue Initial			Vertical Blockade			Horizontal Blockade			Round Serpentine			Square Serpentine		
R	G	B	R	G	B	R	G	B	R	G	B	R	G	B	R	G	B
198	134	106	67	172	158	187	140	120	95	138	128	127	137	136	137	146	143
186	125	96	66	169	152	210	174	152	159	150	143	151	156	152	131	150	144
189	131	109	71	174	153	94	186	173	190	133	114	110	140	132	138	157	151
180	122	98	69	165	153	189	142	124	165	136	118	117	144	139	129	154	148
203	142	113	61	168	150	88	189	173	120	167	159	133	142	139	140	150	142
189	145	116	58	165	149	178	150	138	178	126	105	120	147	140	149	158	155
184	127	97	63	164	148	102	180	164	96	175	153	115	147	136	132	141	138
190	129	108	77	178	162	175	142	125	111	119	121	131	158	151	137	156	152
192	122	96	73	176	159	94	183	165	117	149	138	119	140	133	142	163	158
192	128	101	61	172	155	159	127	106	166	133	114	112	133	126	140	146	144

Table 9.2.7 Raw RGB values at outlet of center serpentine, final gradient mixer

Final Gradient Mixer		
R	G	B
46	94	82
82	90	69
81	113	100
70	103	92
86	91	69
80	101	86
91	93	71
57	103	93
99	103	80
80	88	73

9.3 Appendix – PDMS Lens

9.3.1 Matlab Code

```
% Author: Erika Hancock
% Title: circle_arc_calculations
%
% This code calculates the radius of the lens given the amount the lens
has
% deflected out.

AB = 0.68;
a = AB/2;
x = [0:0.001:a];


for i = 1:length(x)
    radius(i) = (a^2+x(i)^2)/(2*x(i));
end

% Uncomment for manual x displacement calculation
% x_given = 0.075;
% radius_given = (a.^2+x_given.^2)/(2*x_given);
% circ_center = -radius_given+x_given;
% ang = 0:0.01:2*pi;
% xp = radius_given*cos(ang);
% yp = (radius_given*sin(ang))+circ_center;


for k=1:length(x)
    circ_center = -radius(k)+x(k);
    ang = 0:0.01:2*pi;
    xp = radius(k)*cos(ang);
    yp = (radius(k)*sin(ang))+circ_center;
    hold on
    grid on
    axis equal
    line = plot([-a,a],[0,0],'b');
    circle = plot(xp,yp,'r');
    pause(0.5);
    %delete(circle);
end
```

9.4 Appendix – Micro Pin Valves

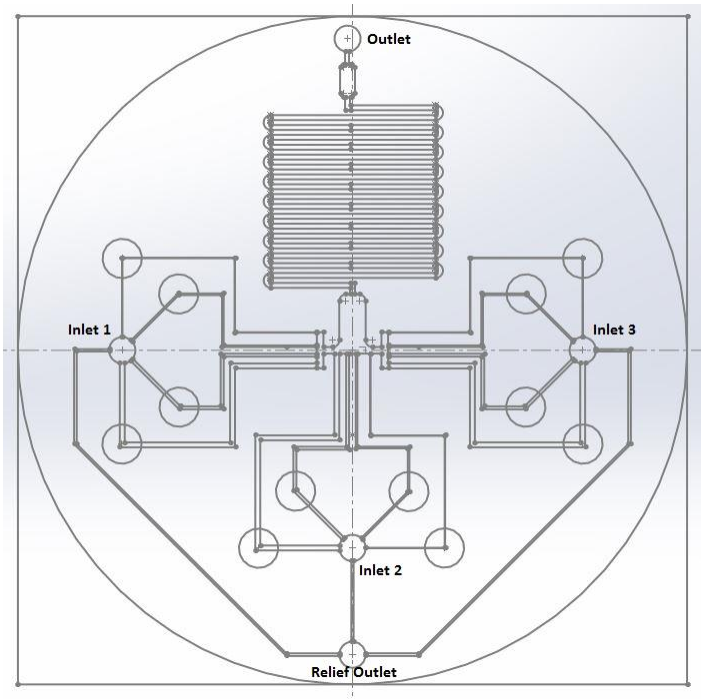

Figure 9.4.1. SolidWorks drawing of proposed final design.

9.5 Appendix-Gantt Charts

	Task Mode	Task Name
1		Understand the nature of our project: microfluidics & scaling phenomenon
2		Determine customer needs
3		Nanofab training course
4		Create a budget
5		Document scaling phenomenon: Generate concepts
6		Determine critical functions
7		Model critical functions
8		Build prototypes
9		CFP motivational Presentation
10		Fabrication
11		Test critical function
12		Review device designs
13		Improve on design
14		CFP presentation

Fall 2015

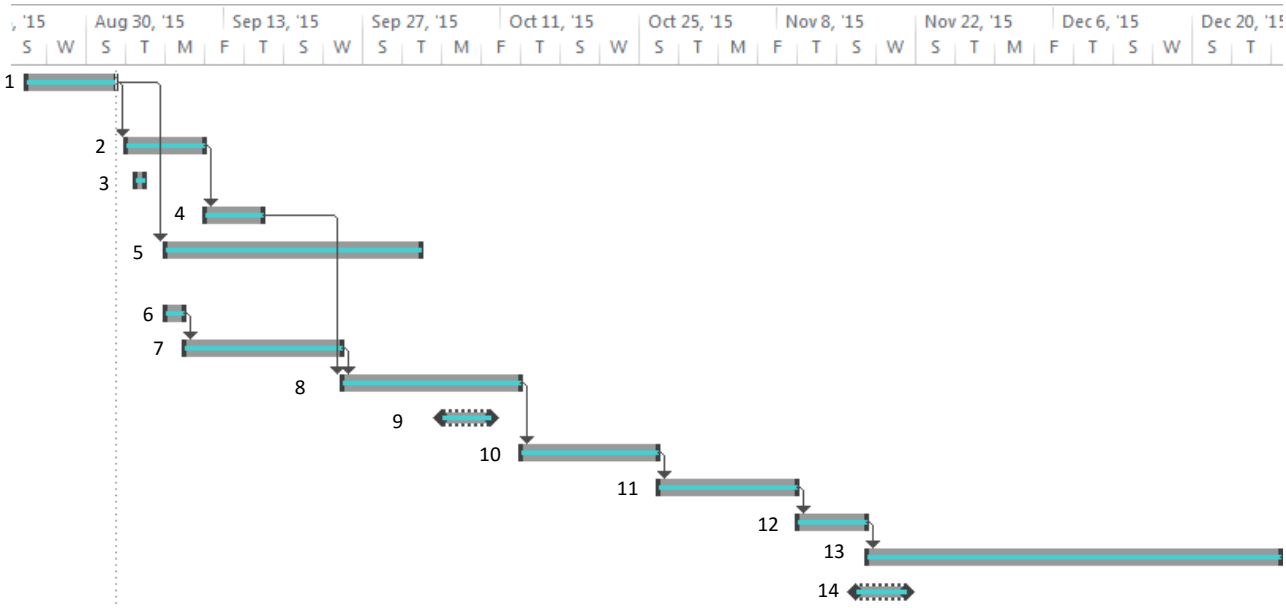

Figure 9.5.1. Gantt chart for fall semester

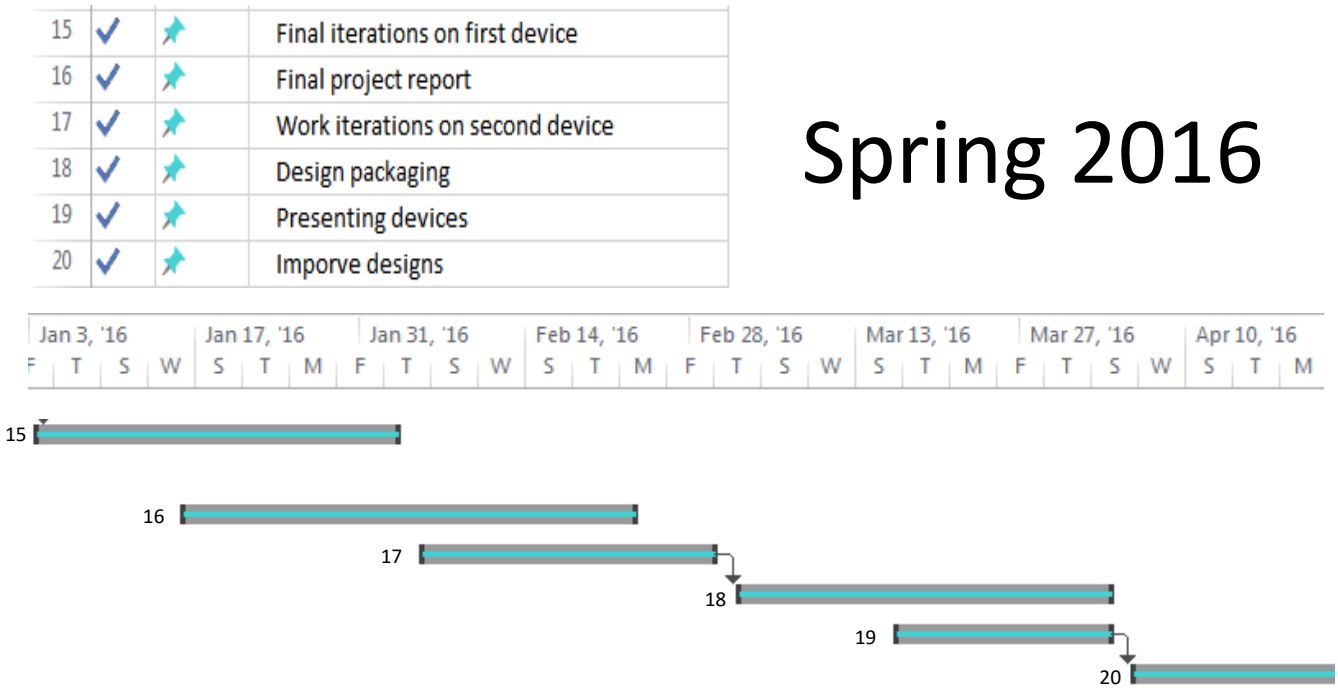

Figure 9.5.2. Gantt chart for spring semester